

CHEMISTRY

A **European** Journal

Supporting Information

9H-Quinolino[3,2,1-k]phenothiazine: A New Electron-Rich Fragment for Organic Electronics

Cyril Poriel,^{*[a]} Joëlle Rault-Berthelot,^{*[a]} Sébastien Thiery,^[a] Cassandre Quinton,^[a]
Olivier Jeannin,^[a] Urelle Biapo,^[b] Denis Tondelier,^[b] and Bernard Geffroy^[b, c]

chem_201603659_sm_miscellaneous_information.pdf

Table of content

MATERIAL AND METHODS.....	1
SYNTHESIS.....	3
THERMAL PROPERTIES.....	25
PHOTOPHYSICAL PROPERTIES	26
ELECTROCHEMICAL PROPERTIES.....	29
THEORETICAL MODELING	31
ORGANIC LIGHT EMITTING DIODES	40
COPIES OF NMR SPECTRA	45

MATERIAL AND METHODS

Synthesis:

Commercially available reagents and solvents were used without further purification other than those detailed below. *n*-Butyllithium 2.5 M solution in hexanes was bought from Sigma-Aldrich®. THF was distilled from sodium/benzophenone prior to use. Light petroleum refers to the fraction with bp 40-60°C. Reactions were stirred magnetically. Analytical thin layer chromatography was carried out using aluminum backed plates coated with Merck Kieselgel 60 GF254 and visualized under UV light (at 254 and 360 nm). Chromatography was carried out using Teledyne Isco CombiFlash® Rf 400 (UV detection 200-360 nm), over standard silica cartridges (conditions of columns is stated in the experimental procedure of each compound). ¹H and ¹³C NMR spectra were recorded using Bruker 300 MHz instruments (¹H frequency, corresponding ¹³C frequency: 75 MHz); chemical shifts were recorded in ppm and J values in Hz. In the ¹³C NMR spectra, signals corresponding to CH, CH₂ or CH₃ groups, assigned from DEPT, are noted; all others are C. The residual signal for the CD₂Cl₂ is 5.32 ppm for the proton and 54.00 ppm for the carbon. The following abbreviations have been used for the NMR assignment: s for singlet, d for doublet, t for triplet and m for multiplet. High resolution mass spectra were recorded at the Centre Régional de Mesures Physiques de l'Ouest (Rennes).

X Ray:

Crystal was picked up with a cryoloop and then frozen at 150 K under a stream of dry N₂ on a APEX II Bruker AXS diffractometer for X-ray data collection (Mo K α radiation, $\lambda = 0.71073 \text{ \AA}$).

The structures were solved by direct methods using the SIR97 program,^[1] and then refined with full-matrix least-square methods based on F2 (SHELXL-97) with the aid of the WINGX^[2] program. All non-hydrogen atoms were refined with anisotropic atomic displacement parameters. H atoms were finally included in their calculated positions. Crystallographic data have been deposited with the Cambridge Crystallographic Data Centre as supplementary publication no. CCDC 1487828 (**SQPTZ-F**) and 1487827 (**SQPTZ-TXO₂**). Copies of the data can be obtained free of charge on application to CCDC, 12 Union Road, Cambridge CB2 1EZ, UK [fax: (+44) 1223-336-033; e-mail: deposit@ccdc.cam.ac.uk].

Figures were drawn using Mercury 3.3 (Build RC5).

Spectroscopic studies:

Cyclohexane (AnalaR NORMAPUR, VWR), acetonitrile (Anhydrous for analysis, Carlo Erba), 2-Methylpentane (99+%, Alfa Aesar), 2-Methyl-THF (analytical anhydrous (ALDRICH)), H₂SO₄ 1N solution in water (Standard solution, Alfa Aesar) and Quinine sulfate dihydrate (99+%, Alfa Aesar) were used without further purification. UV-visible spectra were recorded using a UV-Visible spectrophotometer SHIMADZU UV-1605. The optical gap was calculated from the absorption edge of the UV-vis absorption spectrum using the formula ΔE^{opt} (eV) = hc/λ , λ being the absorption edge (in meter). With $h = 6.62606 \times 10^{-34}$ J.s (1eV = 1.60217×10^{-19} J) and $c = 2.99792 \times 10^8$ m.s⁻¹, this equation may be simplified as: ΔE^{opt} (eV) = $1239.84/\lambda$ (in nm).

Photoluminescence spectra were recorded with a PTI spectrofluorimeter (PTI-814 PDS, MD 5020, LPS 220B) using a xenon lamp. Quantum yields in solution (ϕ_{sol}) were calculated relative to quinine sulfate ($\phi_{\text{sol}} = 0.546$ in H₂SO₄ 1N). ϕ_{sol} was determined according to the following equation (1),

$$\phi_{\text{sol}} = \phi_{\text{ref}} \times 100 \times \frac{(T_s \times A_r)}{(T_r \times A_s)} \left(\frac{n_s}{n_r} \right)^2 \quad (1)$$

where, subscripts s and r refer respectively to the sample and reference. The integrated area of the emission peak in arbitrary units is given as T, n is the refracting index of the solvent and A is the absorbance. 4 solutions of different concentration of the substrate ($A < 0.1$) were prepared and 4 solutions of quinine sulfate, and absorption and emission spectrum were recorded (excitation at 336 nm for the quinine sulfate). Slope of the integrated emission intensity vs. absorbance gave T_x/A_x . 4 quantum yields are then calculated and the average value is reported

Low temperature (77 K) measurements were performed in 2-MethylTHF solution which freezes as a transparent glassy matrix. Measurements were carried using a single-block quartz cuvette containing the solution, which was placed in an Oxford Optistat cryostat cooled with liquid nitrogen, equipped itself with three quartz optical windows.

IR spectra were recorded on a Bruker Vertex 70 using a diamond crystal MIRacle ATR (Pike).

Electrochemical studies:

All electrochemical experiments were performed under an argon atmosphere, using a Pt disk electrode (diameter 1 mm), the counter electrode was a vitreous carbon rod and the reference electrode was a silver wire in a 0.1 M AgNO₃ solution in CH₃CN. Ferrocene was added to the electrolytic solution at the end of a series of experiments. The ferrocene/ferrocenium (Fc/Fc⁺) couple served as internal standard. The three electrode cell was connected to a PAR Model 273 potentiostat/galvanostat (PAR, EG&G, USA) monitored with the ECHEM Software. Activated Al₂O₃ was added in the electrolytic solution to remove excess moisture. For a further comparison of the electrochemical and optical properties, all potentials are referred to the SCE electrode that was calibrated at 0.405 V vs. Fc/Fc⁺ system. Following the work of Jenekhe, we estimated the electron affinity (EA) or lowest unoccupied molecular orbital (LUMO) and the ionization potential (IP) or highest occupied molecular orbital (HOMO) from the redox data. The LUMO level was calculated from: LUMO (eV) = $-[E_{\text{onset}}^{\text{red}} (\text{vs SCE}) + 4.4]$ and the HOMO level from: HOMO (eV) = $-[E_{\text{onset}}^{\text{ox}} (\text{vs SCE}) + 4.4]$, based on an SCE energy level of 4.4 eV relative to the vacuum. The electrochemical gap was calculated from : $\Delta E^{\text{el}} = |\text{HOMO-LUMO}|$ (in eV).^[3-4]

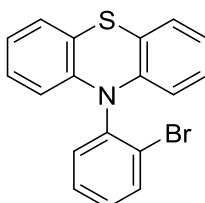
Thermal analysis:

Thermal Gravimetric Analysis (TGA) was carried out at 10°C/min from 0 to 600°C under nitrogen atmosphere. Differential scanning calorimetry (DSC) was carried out by using NETZSCH DSC 200 F3 instrument equipped with an intracooler. DSC traces were measured at 10 °C/min, 2 heating/cooling cycles were succesvly carried out.

Theoretical modeling :

Full geometry optimization with Density functional theory (DFT)^[5-6] and Time-Dependent Density Functional Theory (TD-DFT) calculations were performed with the hybrid Becke-3 parameter exchange^[7-9] functional and the Lee-Yang-Parr non-local correlation functional^[10] (B3LYP) implemented in the Gaussian 09 (Revision B.01) program suite^[11] using the default convergence criterion implemented in the program. The figures were generated with GaussView 5.0. DFT and TD-DFT calculations at the B3LYP level of theory with the 6-31g(d) basis set were performed on the structures obtained by RX. The triplet state energy level (E_T) of the different molecules was calculated from the difference between the total energy of the molecule (B3LYP/6-31g(d)) in their respective optimized singlet and triplet states (optimization at the B3LYP/6-31g(d) level of theory, infrared spectra were calculated on the final geometry to ascertain that a minimum was obtained *i.e.* no negative frequency). Spin density representations were calculated on the geometry obtained by RX with a positive charge +1 (for the cation). Calculations were carried out at the Centre Informatique National de l'Enseignement Supérieur (CINES) in Montpellier under project c2016085032.

SYNTHESIS



10-(2-bromophenyl)-10H-phenothiazine
1

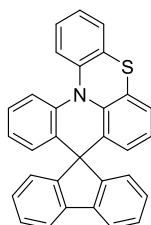
Into a schlenk tube, phenothiazine (10.016 g, 50.263 mmol), 2-bromoiodobenzene (14.365 g, 50.777 mmol, 1.01 eq), potassium phosphate tribasic (30.000 g, 141.329 mmol, 2.81 eq), copper (I) oxide (1.464 g, 10.231 mmol, 0.20 eq) and N^1,N^1,N^2,N^2 -tetramethylethane-1,2-diamine (2.3355 g, 20.098 mmol, 0.40 eq) were dissolved in 1,2-dichlorobenzene (140 mL) under argon. The mixture was heated up to 180°C overnight, and then was allowed to cool down to room temperature. The mixture was quenched with brine (50 mL) and was extracted three times with dichloromethane (3x100 mL). The combine organic extracts were dried over magnesium sulfate, filtered and concentrated under reduce pressure. The residue was purified by flash chromatography on silica gel (light petroleum: dichloromethane 85/15) and recrystallized from ethanol to give the tittle compound as yellow powder. Yield: 41%.

m.p: 97°C; ^1H NMR (300 MHz, CD_2Cl_2) δ : 7.89 (dd, $J = 8.0, 1.4$ Hz, 1H), 7.59 (ddd, $J = 7.8, 7.3, 1.5$ Hz, 1H), 7.51 (dd, $J = 7.8, 1.8$ Hz, 1H), 7.41 (ddd, $J = 8.0, 7.3, 1.9$ Hz, 1H), 7.02 – 6.94 (m, 2H), 6.89 – 6.76 (m, 4H), 6.09 – 5.99 (m, 2H); ^{13}C NMR (75 MHz, CD_2Cl_2) δ : 142.6 (C), 139.7 (C), 135.5 (CH), 134.2 (CH), 130.8 (CH), 130.4 (CH), 127.4 (CH), 127.0 (CH), 126.5 (C), 123.1 (CH), 119.8 (C), 115.7 (CH) ;HRMS calculated for $\text{C}_{18}\text{H}_{13}\text{NBrS}$ 353.9952 $[\text{M}+\text{H}]^+$, found: 353.9948

General procedure for lithiated reaction

10-(2-bromophenyl)-10H-phenothiazine **1** (1 eq) was dissolved in dry THF under argon atmosphere, cooled at -78 °C and stirred during 10 minutes at this temperature. A 2.5M *n*-BuLi solution (1.1 eq) in THF was then slowly injected via a syringe, at -78 °C. The resulting mixture was stirred at the same temperature for 30 min. The corresponding ketone (1.15 eq) dissolved in dry THF was then added dropwise, the mixture was stirred for another 30 minutes at -78°C, and allowed warming up to room temperature gradually overnight. Absolute ethanol (10 mL) was added and the mixture was concentrated under reduced pressure.

Without other purification, the crude was dissolved in methanesulfonic acid and heated up. Then, the mixture was poured onto water/ice (200 mL) and the solution was extracted three times with dichloromethane. The combined organic extracts were dried over magnesium sulfate, filtered, and concentrated under reduced pressure. The residue was purified by flash chromatography on silica gel.

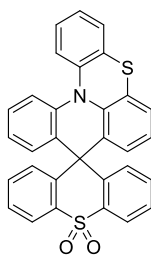


Spiro[fluorene-9,9'-quinolino[3,2,1-kl]phenothiazine] SQPTZ-F

Spiro[fluorene-9,9'-quinolino[3,2,1-kl]phenothiazine] was obtained by following the general procedure, using 10-(2-bromophenyl)-10H-phenothiazine (0.759 g, 2.142 mmol, 1 eq), fluorene-9-one (0.439 g, 2.436 mmol, 1.14 eq), 2.5M *n*-BuLi solution (0.93 mL, 2.325 mmol, 1.09 eq).

Cyclization was done in a mixture of acetic acid and hydrochloric acid (40/4 mL) at reflux for 2 hours. The crude was purified by flash chromatography on silica gel [column conditions: Silica cartridge 24 g (Serlabo); solid deposit on Celite®; $\lambda_{\text{detection}}$: (254 nm and 280 nm); light petroleum/dichloromethane (9/1) at 20 mL/min; collected fraction: 20-35 min]. The product was recrystallized from a mixture of dichloromethane/ethanol (1:1) to give the title compound as a colorless powder. Yield: 80%.

m.p: 220°C; IR (ATR, cm^{-1}): $\nu = 571, 619, 648, 665, 721, 740, 787, 864, 914, 930, 974, 1034, 1113, 1157, 1227, 1252, 1277, 1296, 1315, 1433, 1477, 1579, 1913, 3014, 3062$; ^1H NMR (300 MHz, CD_2Cl_2): δ 7.95 – 7.89 (m, 1H, ArH), 7.78 – 7.71 (m, 1H, ArH), 7.60 – 7.50 (m, 2H, ArH), 7.48 – 7.40 (m, 2H, ArH), 7.38 (dd, $J = 7.7, 1.4$ Hz, 1H, ArH), 7.35 – 7.14 (m, 5H, ArH), 7.14 – 7.07 (m, 2H, ArH), 6.99 (td, $J = 7.5, 1.1$ Hz, 1H, ArH), 6.84 (ddd, $J = 8.0, 7.2, 1.2$ Hz, 1H, ArH), 6.76 (t, $J = 7.7$ Hz, 1H, ArH), 6.55 (dd, $J = 7.9, 1.4$ Hz, 1H, ArH), 6.36 (dd, $J = 7.9, 1.4$ Hz, 1H, ArH); ^{13}C NMR (75 MHz, CD_2Cl_2) δ : 154.3 (C), 150.8 (C), 143.5 (C), 143.0 (C), 139.7 (C), 139.6 (C), 137.7 (C), 133.3 (C), 131.1 (C), 129.01 (CH), 128.99 (CH), 128.93 (CH), 128.7 (CH), 128.28 (CH), 128.25 (CH), 127.9 (CH), 127.48 (CH), 127.47 (CH), 127.3 (C), 126.3 (CH), 125.4 (CH), 125.0 (CH), 124.7 (C), 124.6 (CH), 124.3 (CH), 124.2 (CH), 120.9 (CH), 120.7 (CH), 120.4 (CH), 119.3 (CH), 57.8 (C spiro); HRMS calculated for $\text{C}_{31}\text{H}_{20}\text{NS}$ $[\text{M}+\text{H}]^+$: 438.1316, found: 438.1315; Elemental analysis calculated for $\text{C}_{31}\text{H}_{19}\text{NS}$: C 85.09 %, H 4.38 %, N 3.20 %, S 7.33 %, found: C 84.96 %, H 4.38 %, N 3.37 %, S 7.11 %; λ_{abs} [nm] (ϵ [$10^4 \cdot \text{L} \cdot \text{mol}^{-1} \cdot \text{cm}^{-1}$]) = 240 (3.4), 263 (5.4), 308 (2.5)



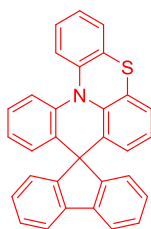
Spiro[quinolino[3,2,1-kl]phenothiazine-9,9'-thioxanthene] 10',10'-dioxide
SQPTZ-TXO₂

Spiro[quinolino[3,2,1-kl]phenothiazine-9,9'-thioxanthene] 10',10'-dioxide was obtained by following the general procedure using 10-(2-bromophenyl)-10H-phenothiazine (1.003 g, 2.831 mmol), 9H-thioxanthene-9-one 10,10-dioxide (0.793 g, 3.246 mmol, 1.15 eq) and a 2.5M solution of *n*-BuLi (1.24 mL, 3.100 mmol, 1.10eq).

Cyclization was done in a mixture of acetic acid and hydrochloric acid (40/4 mL) at reflux for 2 hours. The crude was purified by flash chromatography on silica gel [column conditions: Silica cartridge 24 g (Serlabo); solid deposit on Celite®; λdetection: (254 nm and 280 nm); light petroleum at 18 mL/min; collected fraction: 15-35 min]. Yield: 80%.

mp: 283°C; IR (ATR, cm⁻¹): ν = 536, 571, 592, 644, 719, 731, 750, 787, 868, 1059, 1113, 1146, 1159, 1228, 1248, 1265, 1296, 1323, 1435, 1475, 1489, 1578, 3024, 3062, 3656; ¹H NMR (300 MHz, CD₂Cl₂) δ: 8.22 (ddd, *J* = 8.0, 1.4, 0.4 Hz, 1H), 8.12 (ddd, *J* = 8.0, 1.4, 0.6 Hz, 1H), 7.64 – 7.57 (m, 1H), 7.56 – 7.35 (m, 5H), 7.35 – 7.18 (m, 6H), 7.09 (ddd, *J* = 8.2, 1.2, 0.5 Hz, 1H), 6.95 (ddd, *J* = 8.2, 7.0, 1.3 Hz, 1H), 6.92 – 6.85 (m, 2H), 6.63 (dd, *J* = 8.0, 1.4 Hz, 1H); ¹³C NMR (75 MHz, CD₂Cl₂) δ: 145.0 (C), 143.7 (C), 143.3 (C), 138.9 (C), 137.4 (C), 137.1 (C), 134.9 (CH), 134.6 (C), 133.9 (CH), 133.8 (C), 133.1 (CH), 132.9 (C), 131.9 (CH), 131.1 (CH), 130.0 (CH), 129.2 (CH), 129.0 (CH), 128.7 (CH), 128.3 (CH), 128.2 (CH), 127.8 (C), 127.2 (CH), 125.4 (CH), 125.2 (CH), 125.0 (CH), 124.8 (C), 123.3 (CH), 122.2 (CH), 121.4 (CH), 119.2 (CH), 49.2 (C spiro) ; HRMS calculated for C₃₁H₂₀NO₂S₂ [M+H]⁺: 502.0935, found 502.0933; Elemental analysis calculated for C₃₁H₁₉NO₂S₂: C 74.23%, H 3.82%, N 2.79%, O 6.38, S 12.78 %, found: C 74.30 %, H 3.87, N 3.05, O 6.55, S 12.90.

Structural properties



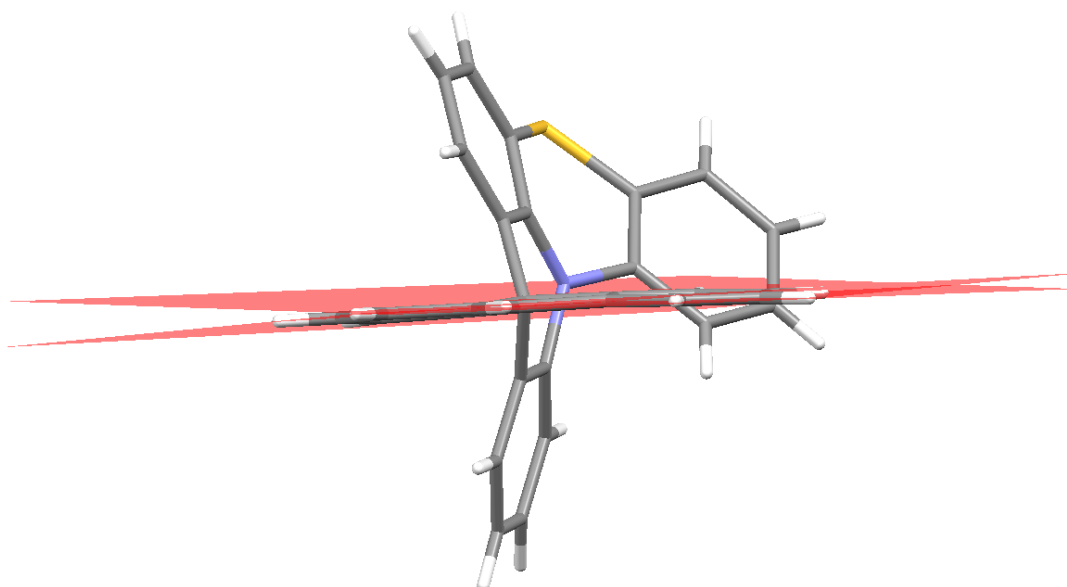
SQPTZ-F

Table 1 Crystal data and structure refinement for SQPTZ-F

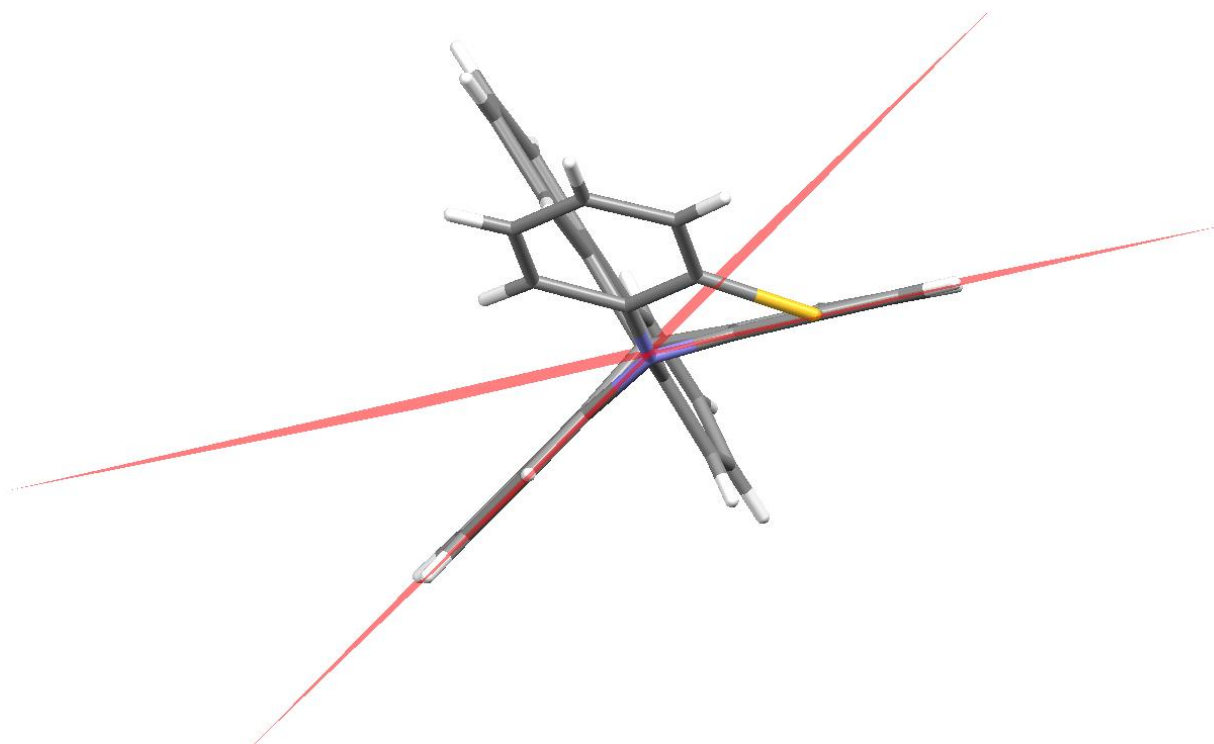
Identification code	SQPTZ-F
Empirical formula	C ₆₂ H ₃₈ N ₂ S ₂
Extended formula	2(C ₃₁ H ₁₉ NS)
Formula weight	875.06
Temperature	150(2) K
Wavelength	0.71073 Å
Crystal system, space group	monoclinic, P ² ₁ /a
Unit cell dimensions	a = 8.9455(12) Å, α = 90 °
	b = 23.946(4) Å, β = 98.420(5) °
	c = 20.453(3) Å, γ = 90 °
Volume	4334.0(11) Å ³
Z, Calculated density	4, 1.341 (g.cm ⁻³)
Absorption coefficient	0.17 mm ⁻¹
F(000)	1824
Crystal size	0.11 x 0.1 x 0.01 mm
Crystal color	colorless
Theta range for data collection	1.01 to 27.55 °
h_min, h_max	-11, 11
k_min, k_max	-31, 31
l_min, l_max	-26, 26
Reflections collected / unique	37464 / 9921 [R(int) = 0.1417]
Reflections [I > 2σ]	4820
Completeness to theta_max	0.991

Absorption correction type	multi-scan
Max. and min. transmission	0.998 , 0.981
Refinement method	Full-matrix least-squares on F ²
Data / restraints / parameters	9921 / 0 / 595
bGoodness-of-fit	1.027
Final R indices [I>2σ]	<i>R1 = 0.0987, wR2 = 0.248</i>
R indices (all data)	<i>R1 = 0.1937, wR2 = 0.3069</i>
Largest diff. peak and hole	0.802 and -0.502 e ⁻ .Å ⁻³

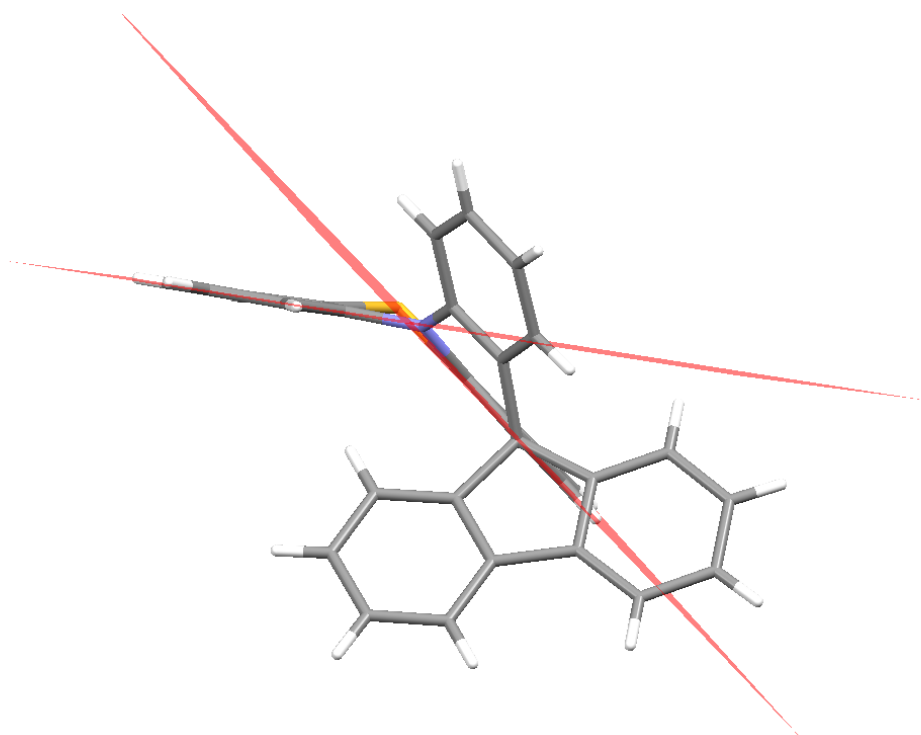
SQPTZ -F X-Ray structure: Molecule 1



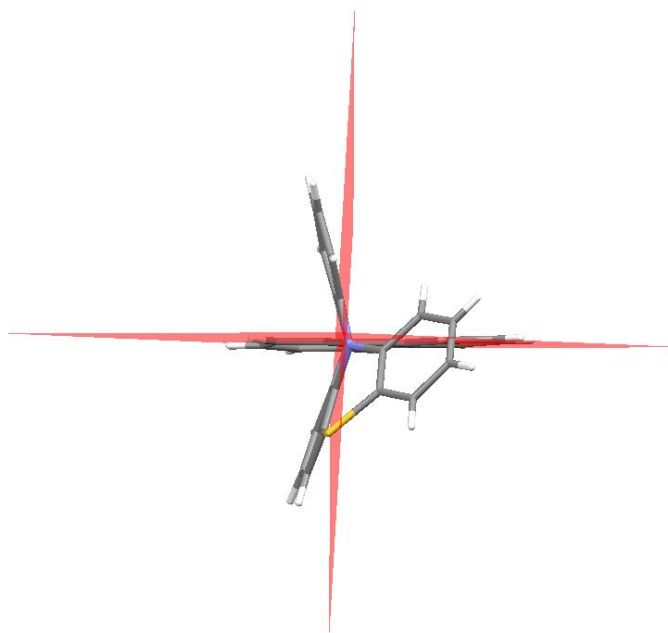
**S 1 Angle between the two phenyl units of the fluorenyl fragment in SQPTZ-F molecule 1:
3.5 °**



**S 2 Angle between the two phenyl units of the acridine fragment in SQPTZ-F molecule 1:
32.9 °**



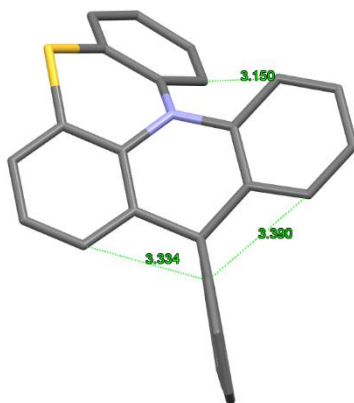
**S 3 Angle between the two phenyl units of the phenothiazine fragment in SQPTZ-F
molecule 1: 37.9 °**



S 4 Angle between the mean plane of cyclopentane in fluorene fragment and the mean plane of cyclohexadiene in acridine fragment in SQPTZ-F molecule 1: 88 °

Intramolecular contacts:

- 3 short C/C intramolecular distances are observed ($d_{C/C}=3.33 \text{ \AA}$, $d_{C/C}=3.15 \text{ \AA}$ and $d_{C/C}=3.39 \text{ \AA}$, see below) in the molecule 1. These short distances are shorter than the sum of the Van der Waals radii, ie $d=3.4 \text{ \AA}$ (according to Bondi, A. J. Phys. Chem. 1964, 68, 441).

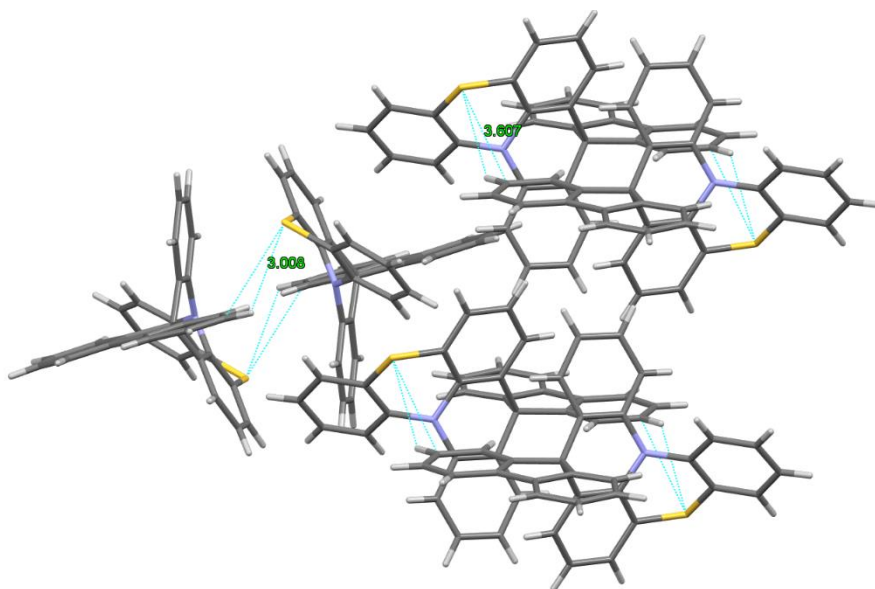


S 5 Short intramolecular contacts in SQPTZ-F molecule 1

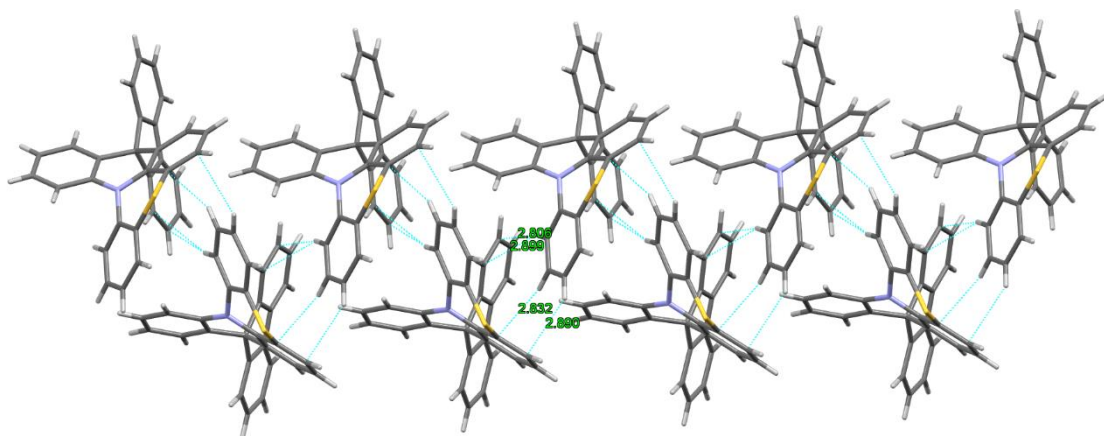
Intermolecular contacts:

- 1 S/H short intermolecular contact is observed ($d_{S/H}=3.00 \text{ \AA}$, see below) in the molecule 1. This short distance is equal to the sum of the Van der Waals radii, ie $d=3.0 \text{ \AA}$ (according to Bondi, A. J. Phys. Chem. 1964, 68, 441).

- 1 S/C intermolecular contact is observed ($d_{S/C}=3.60 \text{ \AA}$, see below) in the molecule 1. This distance is slightly longer than the sum of the Van der Waals radii, ie $d=3.5 \text{ \AA}$ (according to Bondi, A. J. Phys. Chem. 1964, 68, 441).

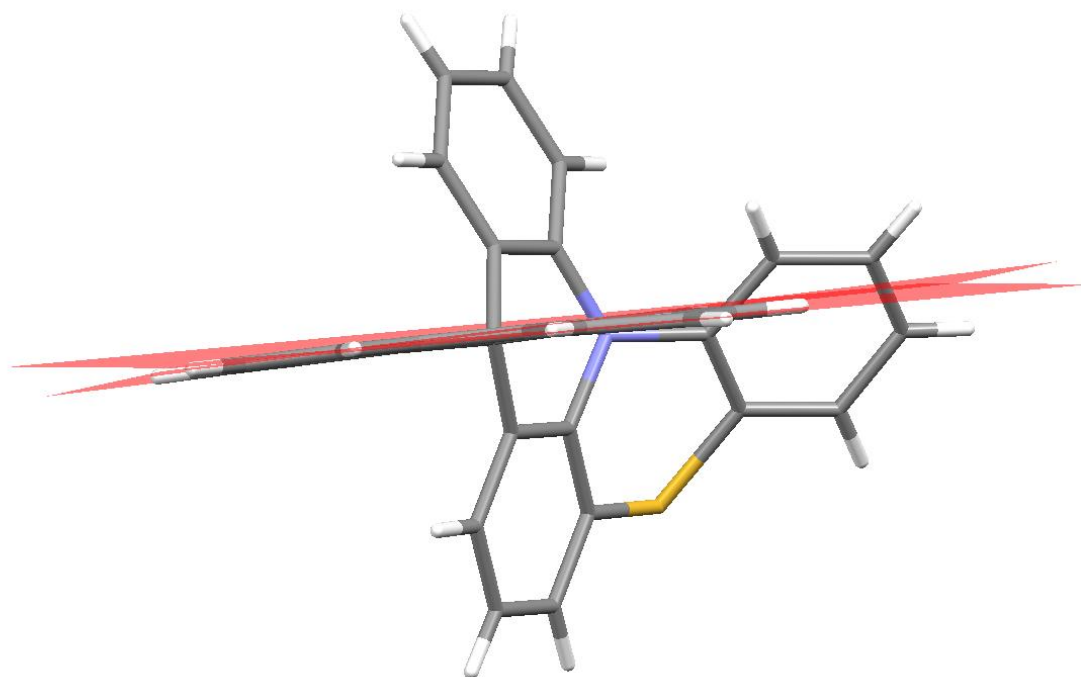


- 4 C/H intermolecular distances are observed ($d_{C/H}=2.81 \text{ \AA}$, $d_{C/H}=2.90 \text{ \AA}$, $d_{C/H}=2.83 \text{ \AA}$ and $d_{C/H}=2.89 \text{ \AA}$, see below) in the molecule 1. These distances are shorter than the sum of the Van der Waals radii, ie $d=2.90 \text{ \AA}$ (according to Bondi, A. J. Phys. Chem. 1964, 68, 441).

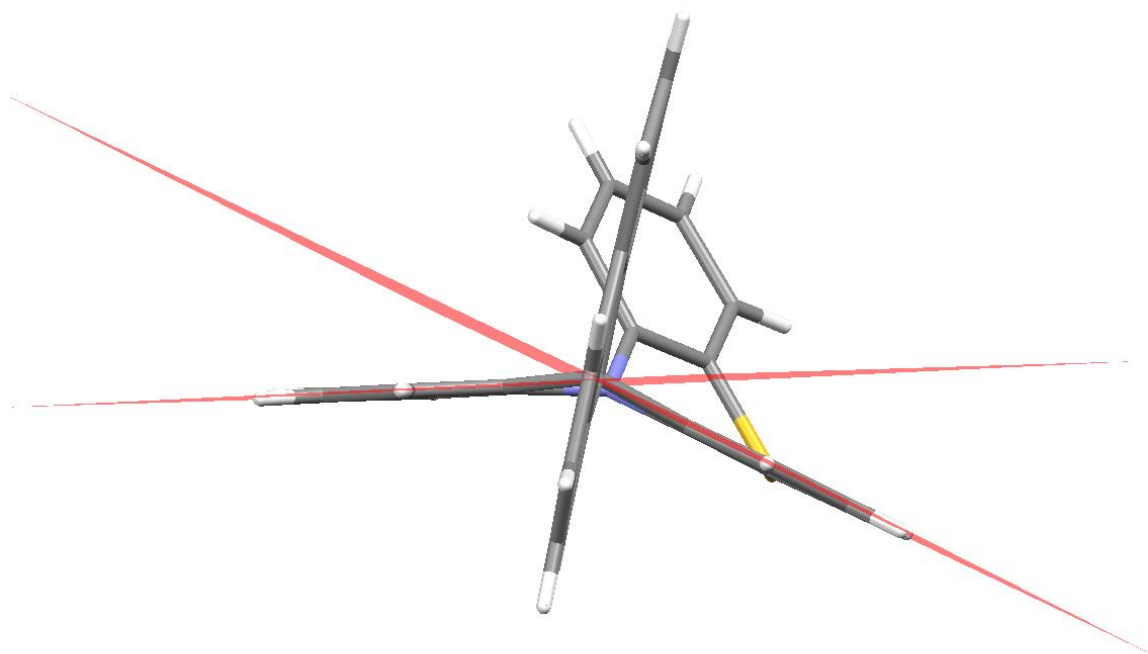


S 6 Short intra and intermolecular contacts in SQPTZ-F molecule 1

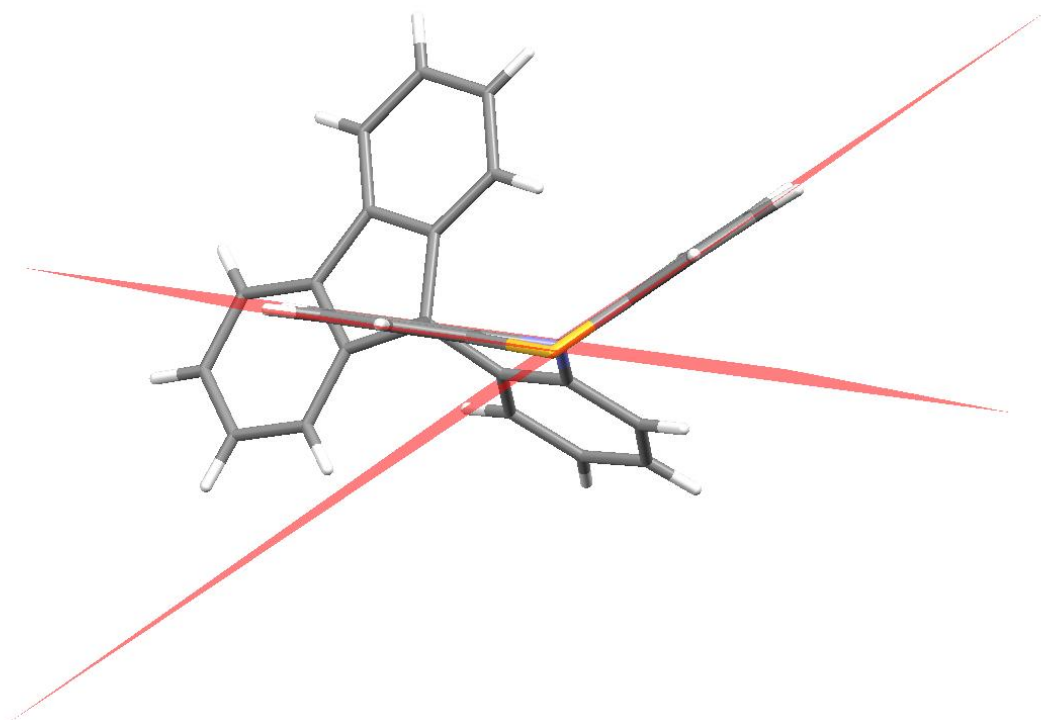
SQPTZ-F X-Ray structure: Molecule 2



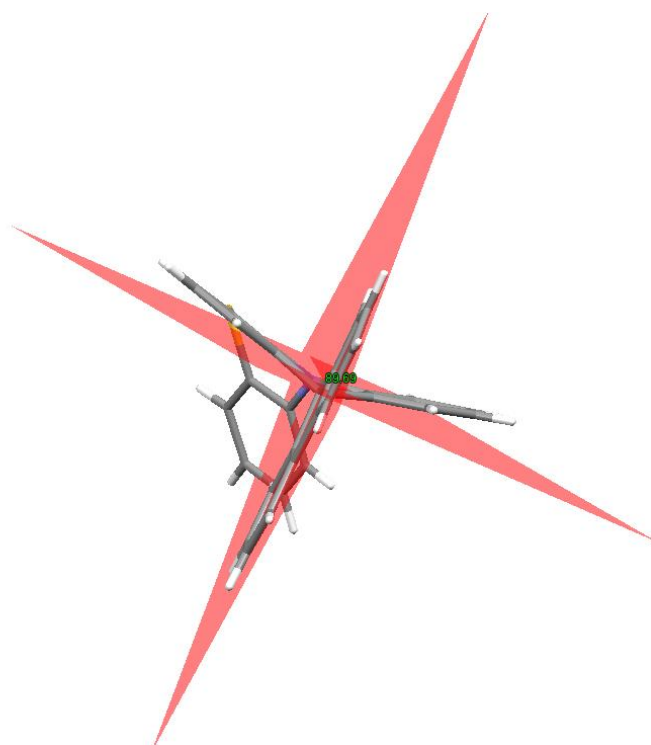
**S 7 Angle between the two phenyl units of the fluorenyl fragment in SQPTZ -F molecule 2:
2.4 °**



**S 8 Angle between the two phenyl units of the acridine fragment in SQPTZ -F molecule 2:
28.5 °**



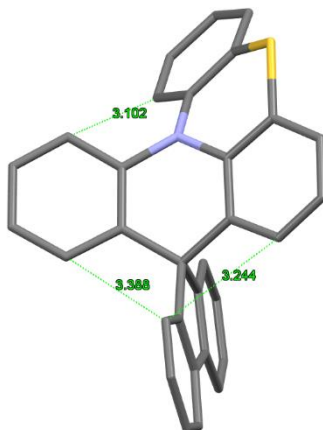
S 9 Angle between the two phenyl units of the phenthiazine fragment in SQPTZ -F molecule 2: 42.3 °



S 10 Angle between the mean plane of cyclopentane in the fluorene fragment and the mean plane of cyclohexadiene in acridine fragment in SQPTZ -F molecule 2: 90 °

Intramolecular contacts:

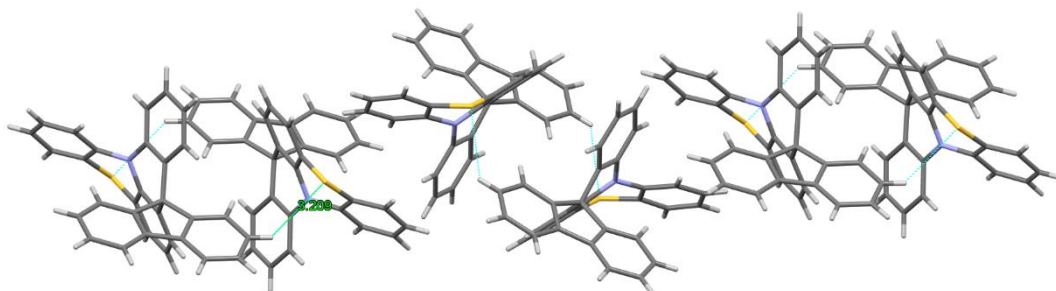
-3 short C/C intramolecular distances are observed ($d_{C/C}=3.24 \text{ \AA}$, $d_{C/C}=3.10 \text{ \AA}$ and $d_{C/C}=3.39 \text{ \AA}$, see below) in the molecule 2. These short distances are shorter than the sum of the Van der Waals radii, ie $d=3.4 \text{ \AA}$ (according to Bondi, A. J. Phys. Chem. 1964, 68, 441).



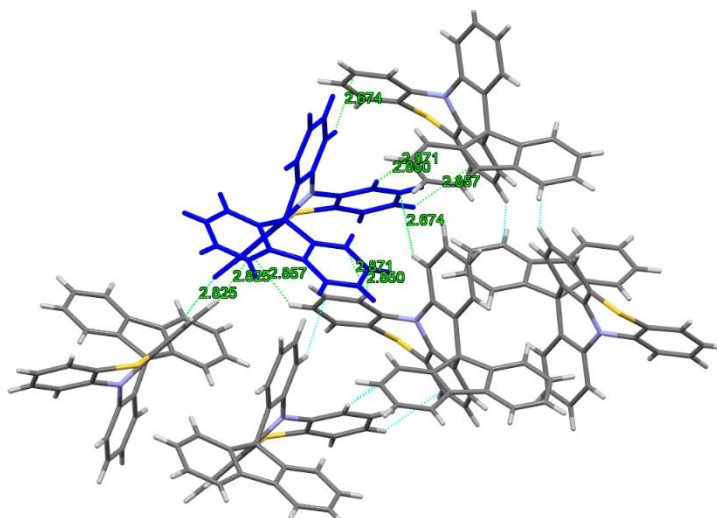
S 11 Short intramolecular contacts in SQPTZ-F molecule 2

Intermolecular contacts:

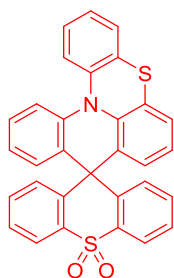
- 1 S/H intermolecular contact is observed ($d_{S/H}=3.21 \text{ \AA}$, see below) in the molecule 2. This distance is nevertheless slightly longer than the sum of the Van der Waals radii, ie $d=3.0 \text{ \AA}$ (according to Bondi, A. J. Phys. Chem. 1964, 68, 441).



- 5 C/H intermolecular distances are observed ($d_{C/H}=2.82 \text{ \AA}$, $d_{C/H}=2.86 \text{ \AA}$, $d_{C/H}=2.85 \text{ \AA}$, $d_{C/H}=2.87 \text{ \AA}$ and $d_{C/H}=2.67 \text{ \AA}$, see below) in the molecule 2. These distances are shorter than the sum of the Van der Waals radii, ie $d=2.90 \text{ \AA}$ (according to Bondi, A. J. Phys. Chem. 1964, 68, 441).



S 12 Short intermolecular contacts in SQPTZ-F molecule 2

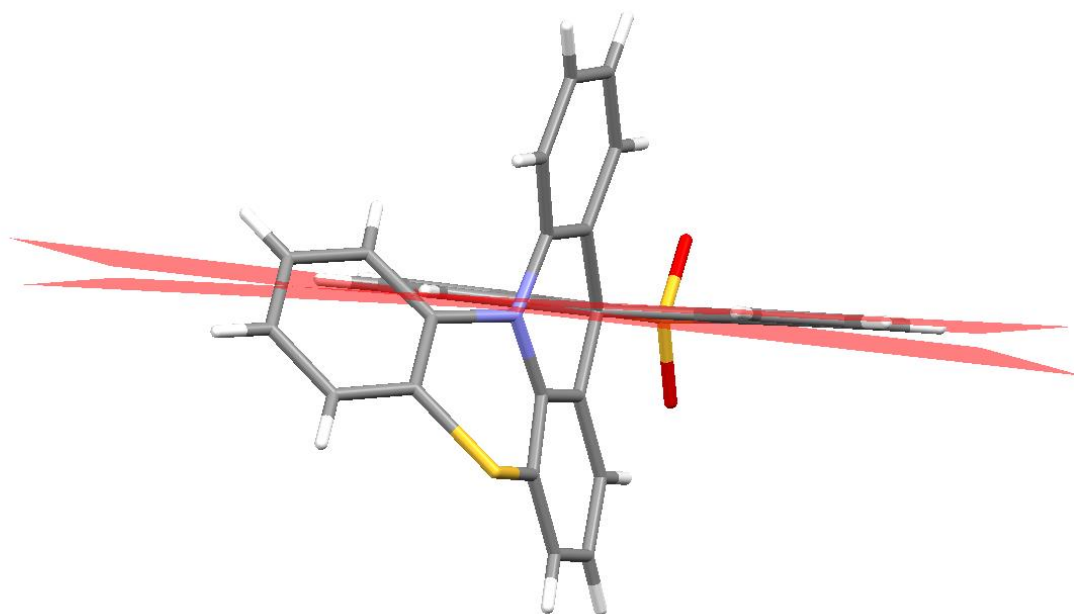


SQPTZ-TXO₂

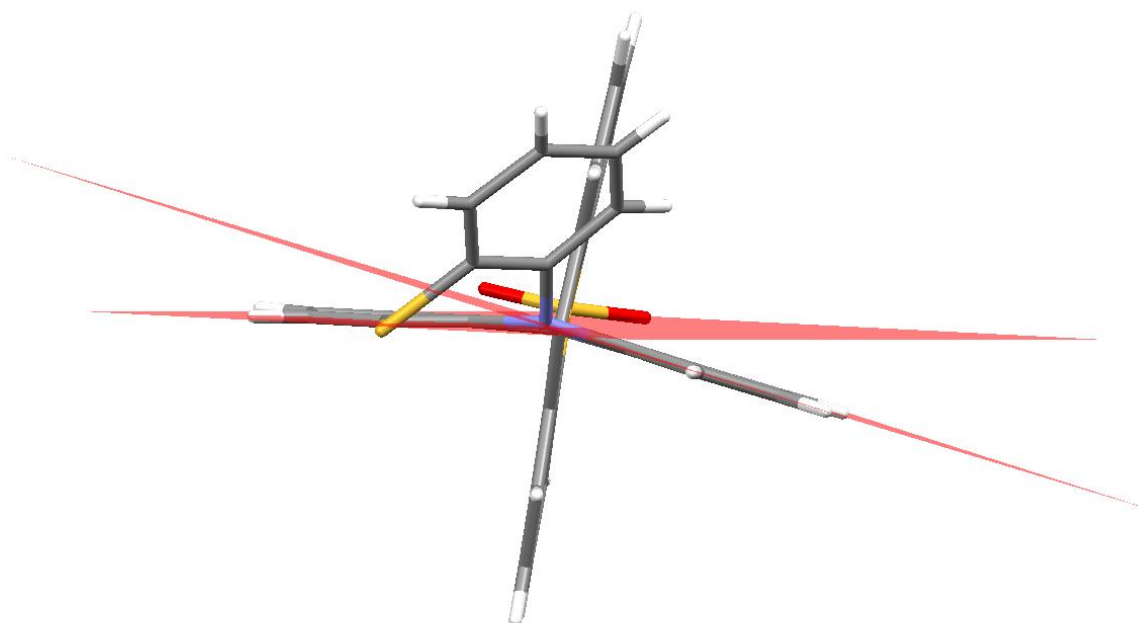
Table 2 Crystal data and structure refinement for SQPTZ-TXO₂

Identification code	SQPTZ-TXO ₂	
Empirical formula	C _{31,5} H _{20,5} ClNO ₂ S ₂	
Extended formula	C ₃₁ H ₁₉ NO ₂ S ₂ , C ₃₁ H ₂₀ NO ₂ S ₂ , CH ₂ Cl ₂	
Formula weight	544.05	
Temperature	150(2) K	
Wavelength	0.71073 Å	
Crystal system, space group	triclinic, <i>P</i> -1	
Unit cell dimensions	a = 8.4549(4) Å, α = 76.751(2) ° b = 12.0556(6) Å, β = 80.657(2) ° c = 25.2183(15) Å, γ = 86.893(2) °	
Volume	2468.5(2) Å ³	
Z, Calculated density	4, 1.464 (g.cm ⁻³)	
Absorption coefficient	0.357 mm ⁻¹	
F(000)	1124	
Crystal size	0.12 x 0.03 x 0.02 mm	
Crystal color	colorless	
Theta range for data collection	0.84 to 27.53 °	
h_min, h_max	-10, 10	
k_min, k_max	-15, 15	
l_min, l_max	-32, 32	
Reflections collected / unique	26401 / 11229 [R(int) = 0.0527]	
Reflections [I>2σ]	7117	
Completeness to theta_max	0.988	
Absorption correction type	multi-scan	
Max. and min. transmission	0.993 , 0.987	
Refinement method	Full-matrix least-squares on F ²	
Data / restraints / parameters	11229 / 0 / 698	
Goodness-of-fit	1.023	
Final R indices [I>2σ]	R1 = 0.0587, wR2 = 0.1483	
R indices (all data)	R1 = 0.1037, wR2 = 0.1897	
Largest diff. peak and hole	0.915 and -1.168 e ⁻ .Å ⁻³	

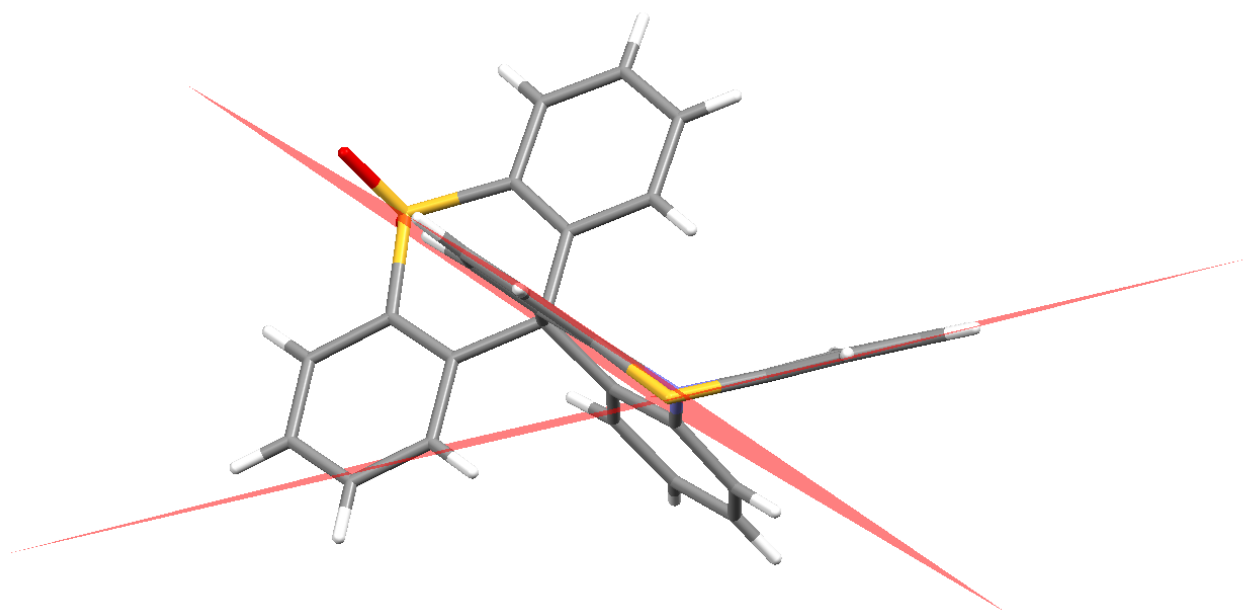
SQPTZ-TXO₂ molecule 1 X-Ray structure



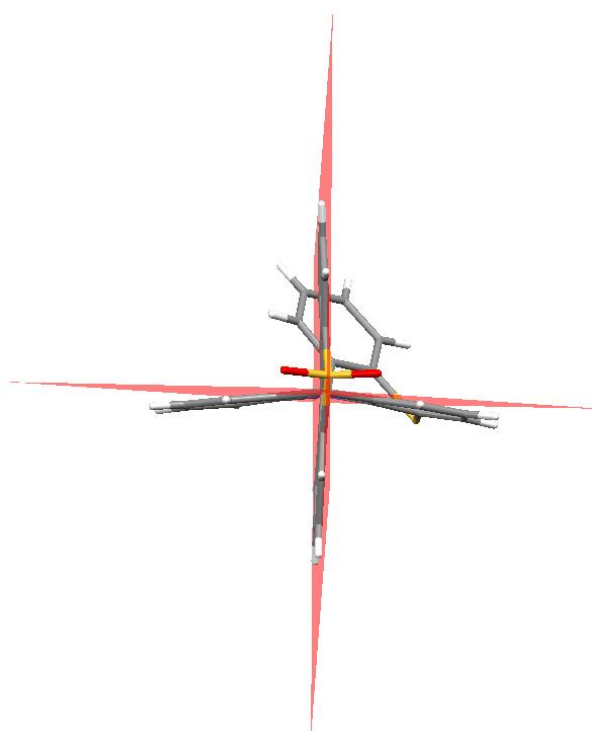
S 13 Angle between the two phenyl units of the dioxothioxanthene fragment in SQPTZ - TXO₂ molecule 1: 4.3 °



S 14 Angle between the two phenyl units of the acridine fragment in SQPTZ -TXO₂ molecule 1: 15.1 °



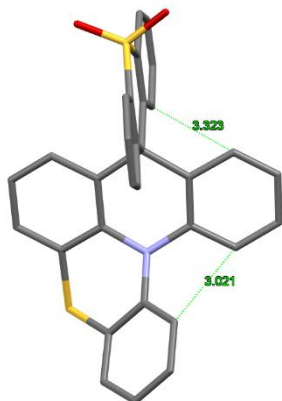
S 15 Angle between the two phenyl units of the phenothiazine fragment in SQPTZ -TXO₂ molecule 1: 46.9 °



S 16 Angle between the mean plane of cyclohexadiene in dioxothioxanthene fragment and the mean plane of cyclohexadiene in acridine fragment in SQPTZ -TXO₂ molecule 1: 89 °

Intramolecular contacts:

-2 very short C/C intramolecular distances are observed ($d_{C/C}=3.32 \text{ \AA}$ and $d_{C/C}=3.02 \text{ \AA}$, see below) in the molecule 1. These short distances are shorter than the sum of the Van der Waals radii, ie $d=3.4 \text{ \AA}$ (according to Bondi, A. J. Phys. Chem. 1964, 68, 441).

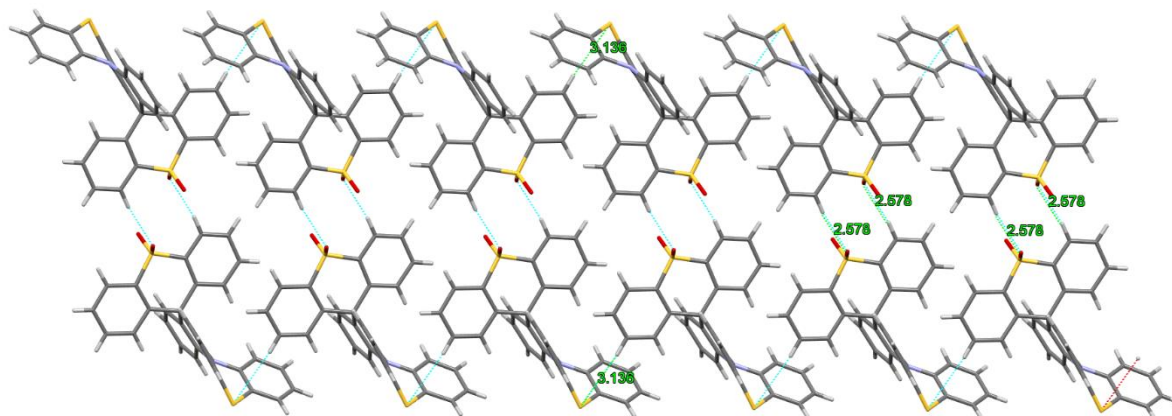


S 17 Short intramolecular contacts in SQPTZ-TXO₂ molecule 1

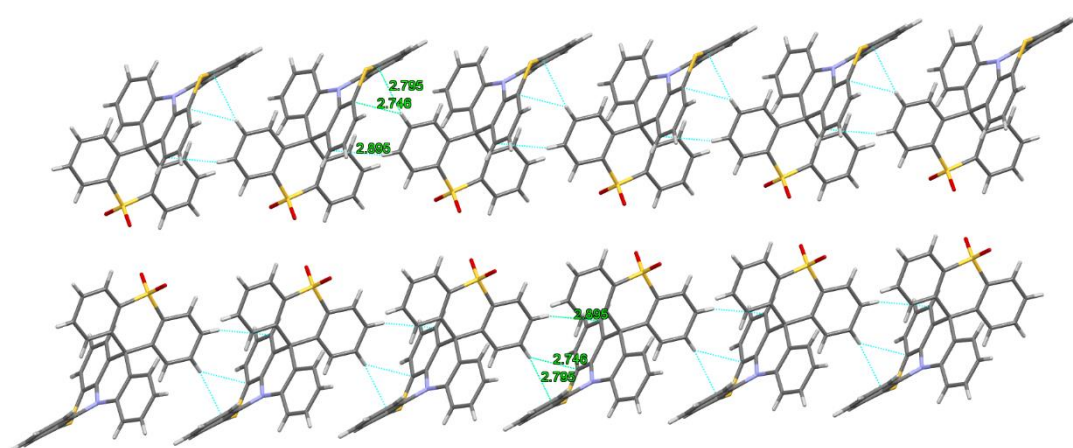
Intermolecular contacts:

- 1 S/H intermolecular contact is observed ($d_{S/H}=3.13 \text{ \AA}$, see below) in the molecule 1. This distance is slightly longer than the sum of the Van der Waals radii, ie $d=3.0 \text{ \AA}$ (according to Bondi, A. J. Phys. Chem. 1964, 68, 441).

- 1 O/H intermolecular distance is observed ($d_{O/H}=2.58 \text{ \AA}$, see below) in the molecule 1. This distance is shorter than the sum of the Van der Waals radii, ie $d=2.72 \text{ \AA}$ (according to Bondi, A. J. Phys. Chem. 1964, 68, 441).

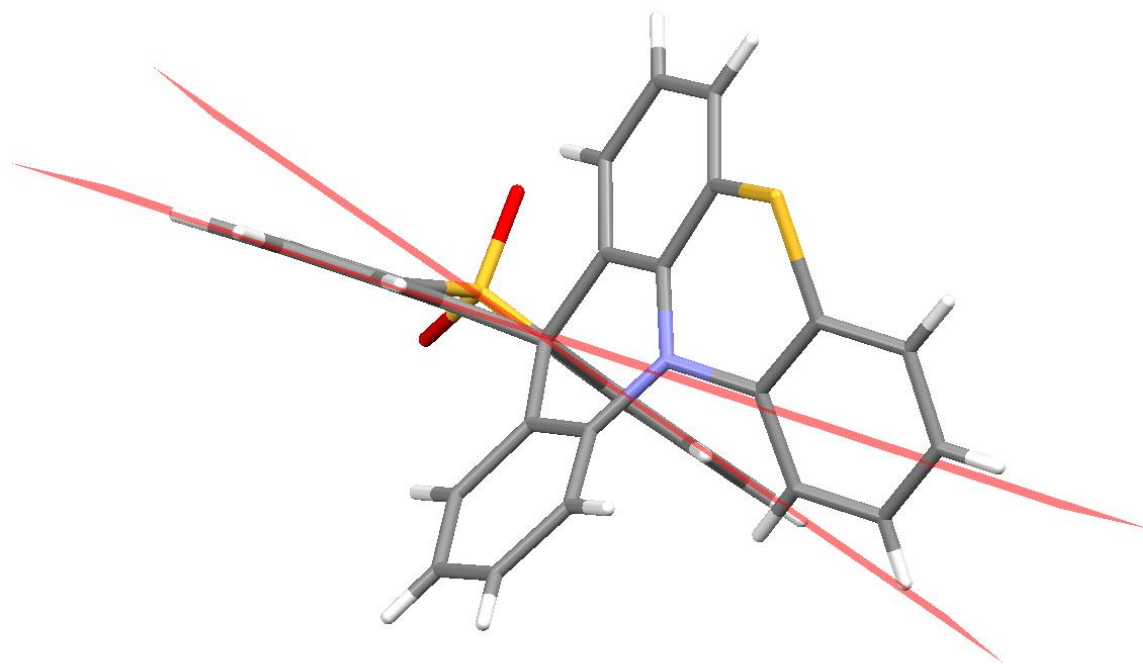


- 3 C/H intermolecular distances are observed ($d_{C/H}=2.79 \text{ \AA}$, $d_{C/H}=2.75 \text{ \AA}$, $d_{C/H}=2.89 \text{ \AA}$, see below) in the molecule 2. These distance are all shorter than the sum of the Van der Waals radii, ie $d=2.90 \text{ \AA}$ (according to Bondi, A. J. Phys. Chem. 1964, 68, 441).



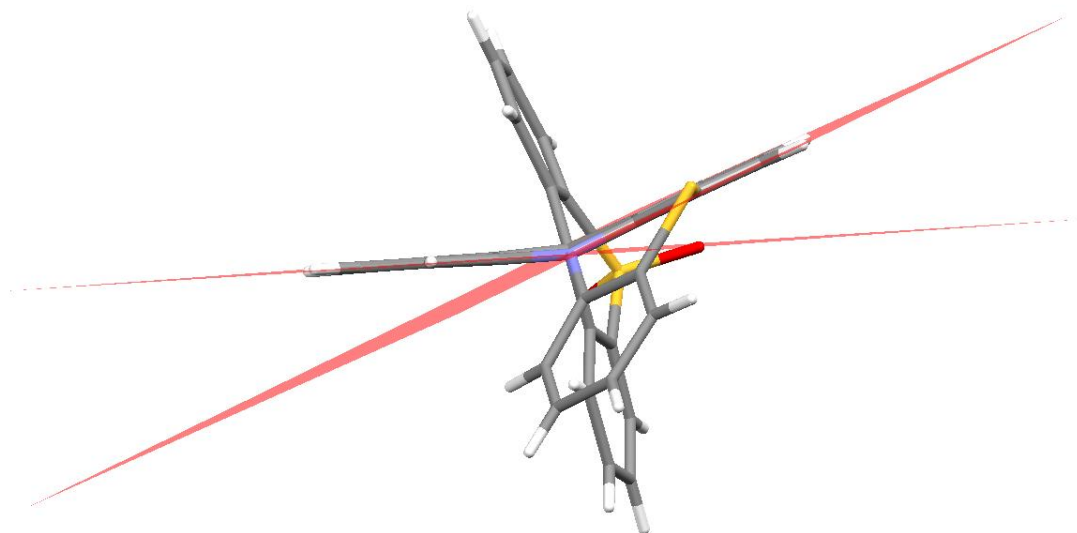
S 18 Short intermolecular contacts in SQPTZ-TXO₂ molecule 1

SQPTZ-TXO₂ molecule 2 X-Ray structure

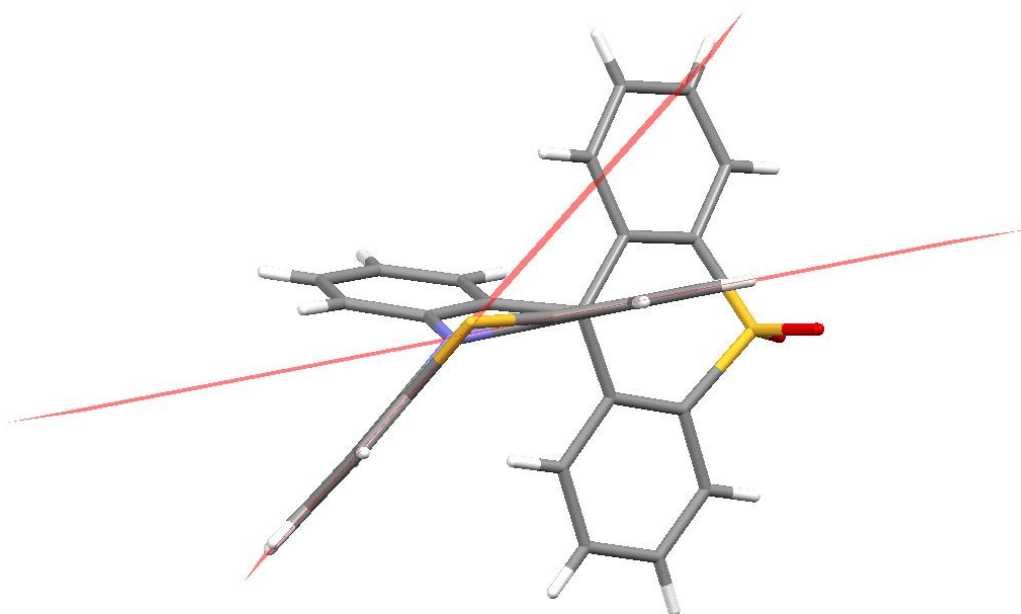


S 13

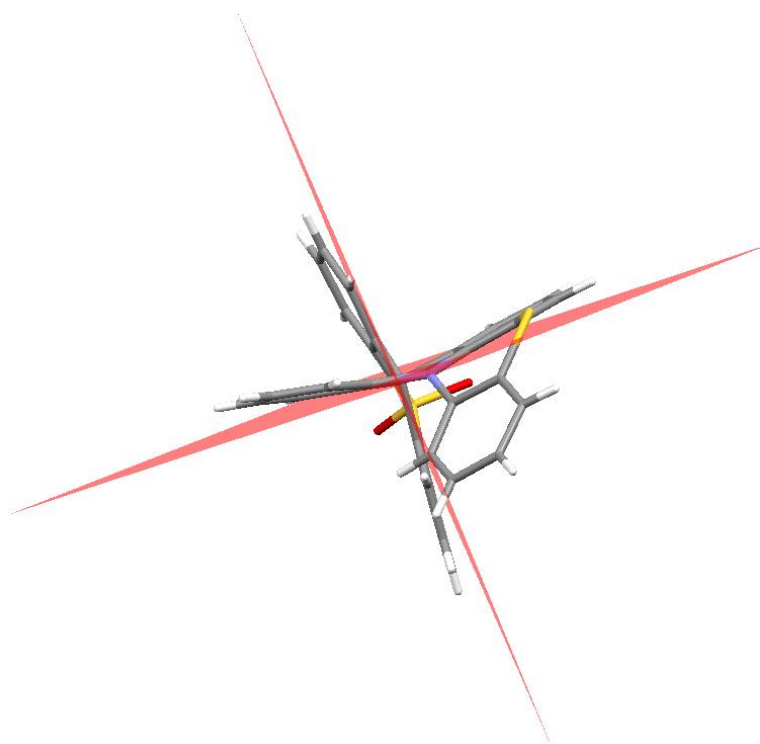
S 19 Angle between the two phenyl units of the dioxothioxanthene fragment in SQPTZ - TXO₂ molecule 2: 16.5 °



S 20 Angle between the two phenyl units of the acridine fragment in SQPTZ -TXO₂ molecule 2: 21.6 °



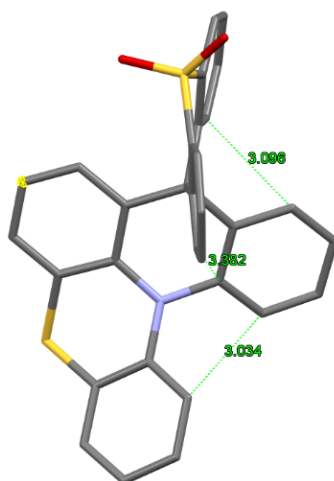
S 21 Angle between the two phenyl units of the phenothiazine fragment in SQPTZ -TXO₂ molecule 2: 37.4 °



S 22 Angle between the mean plane of cyclohexadiene in dioxothioxanthene fragment and the mean plane of cyclohexadiene in acridine fragment in SQPTZ -TXO₂ molecule 2: 86 °

Intramolecular contacts:

-Three very short C/C intramolecular distances are observed ($d_{C/C}=3.09 \text{ \AA}$, $d_{C/C}=3.38 \text{ \AA}$ and $d_{C/C}=3.03 \text{ \AA}$, see below) in the molecule 2. These short distances are shorter than the sum of the Van der Waals radii, ie $d=3.4 \text{ \AA}$ (according to Bondi, A. J. Phys. Chem. 1964, 68, 441).

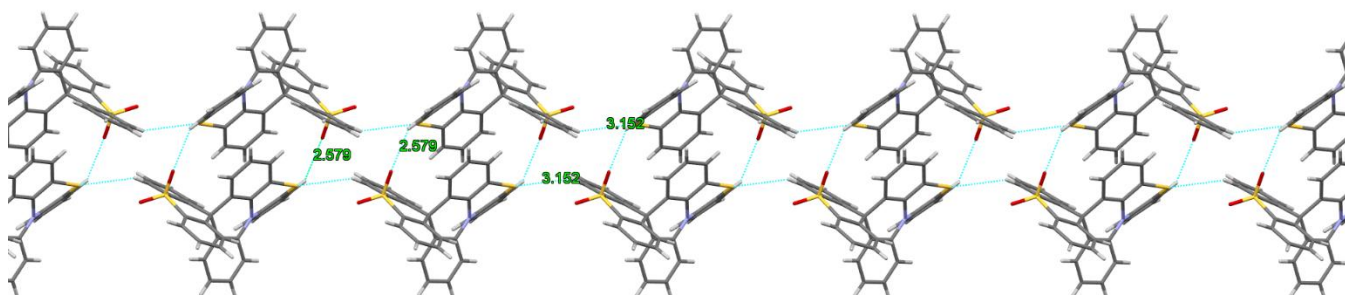


S 23 Short intramolecular contacts in SQPTZ-TXO₂ molecule 2

Intermolecular contacts:

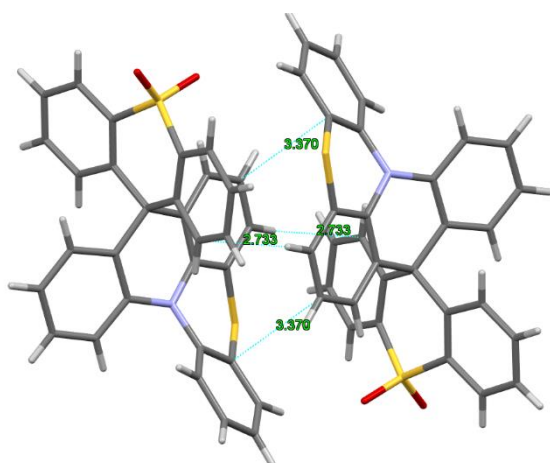
- 1 S/H intermolecular contact is observed ($d_{S/H}=3.15 \text{ \AA}$, see below) in the molecule 2. This distance is slightly longer than the sum of the Van der Waals radii, ie $d=3.0 \text{ \AA}$ (according to Bondi, A. J. Phys. Chem. 1964, 68, 441).

- 1 O/H intermolecular distance is observed ($d_{O/H}=2.58 \text{ \AA}$, see below) in the molecule 2. This distance is shorter than the sum of the Van der Waals radii, ie $d=2.72 \text{ \AA}$ (according to Bondi, A. J. Phys. Chem. 1964, 68, 441).



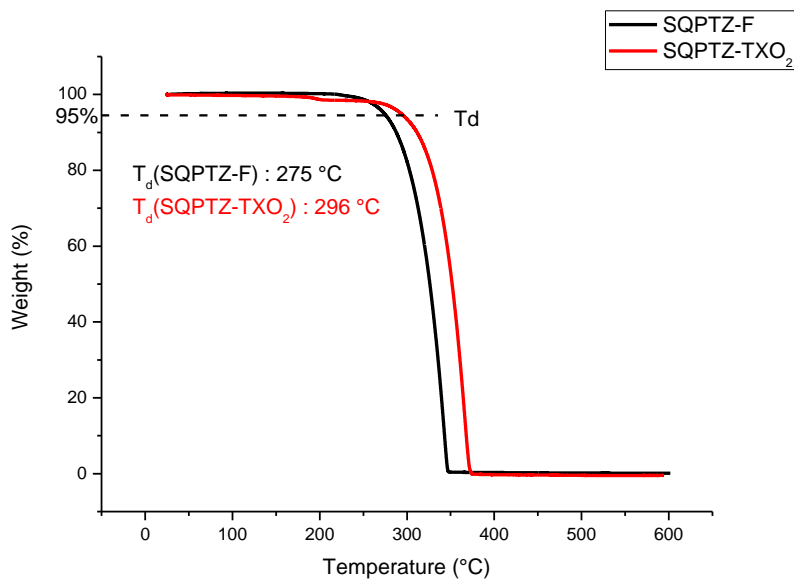
- 1 C/C short intermolecular contact is observed ($d_{C/C}=3.37 \text{ \AA}$, see below) in the molecule 2. This distance is shorter than the sum of the Van der Waals radii, ie $d=3.4 \text{ \AA}$ (according to Bondi, A. J. Phys. Chem. 1964, 68, 441).

- 1 C/H intermolecular distance is observed ($d_{C/H}=2.73 \text{ \AA}$, see below) in the molecule 2. This distance is shorter than the sum of the Van der Waals radii, ie $d=2.90 \text{ \AA}$ (according to Bondi, A. J. Phys. Chem. 1964, 68, 441).

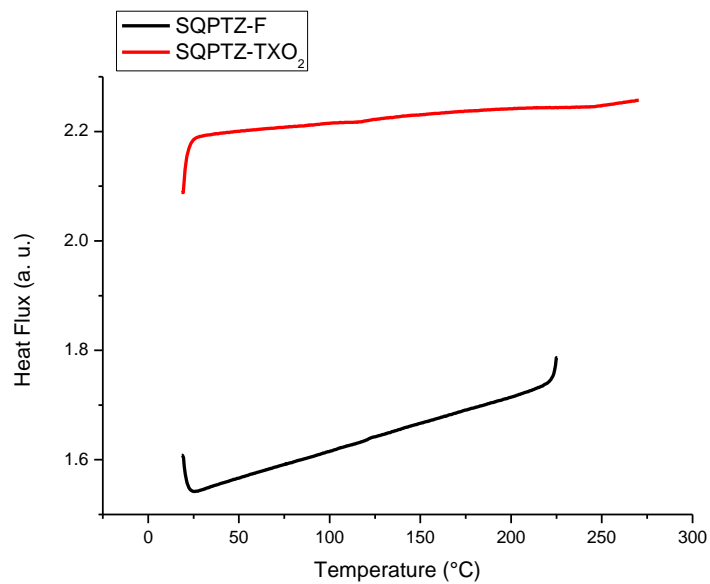


S 24 Short intermolecular contacts in SQPTZ-TXO₂ molecule 2

THERMAL PROPERTIES



S 25 TGA curves of **SQPTZ-F** and **SQPTZ-TXO₂**



S 26 DSC curves of **SQPTZ-F** and **SQPTZ-TXO₂**

PHOTOPHYSICAL PROPERTIES

Solvatochromism

Lippert-Mataga-Ooshika formalism^[12-14] is presented below:

$$\Delta\nu = \frac{2(\Delta\mu)^2}{r^3hc} \Delta f + C \quad \text{with} \quad \Delta f = \left(\frac{\varepsilon - 1}{2\varepsilon + 1} - \frac{n^2 - 1}{2n^2 + 1} \right)$$

With :

" $\Delta\nu$ " (cm^{-1}) being the Stokes shift,

" $\Delta\mu$ " (D) the dipole moment difference between S_0 and S_1 states ($\Delta\mu = \mu^* - \mu$)

" r " (cm) the radius of the solvation sphere calculated from Xray structure,

" h " Planck constant ($6,626 \cdot 10^{-27} \text{erg} \cdot \text{s}^{-1}$),

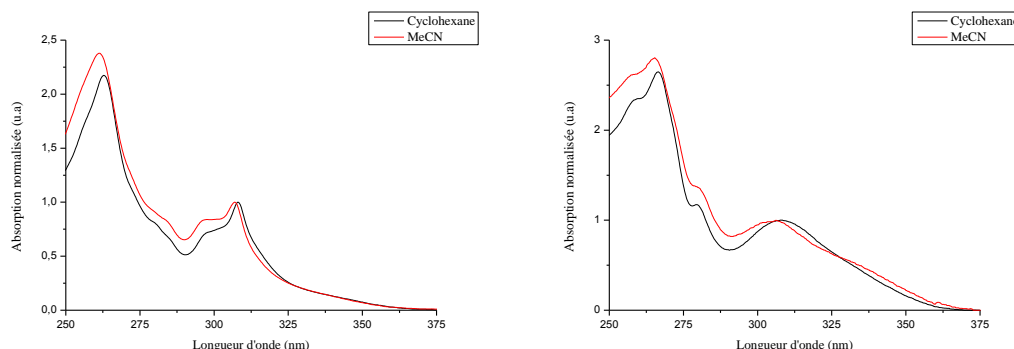
" c " celerity ($2,998 \cdot 10^{10} \text{cm} \cdot \text{s}^{-1}$)

" Δf " is the orientation polarisability of the solvent calculated from its dielectric constant " ε " and its refractive index " n " $\Delta f = (\varepsilon - 1)/(2\varepsilon + 1) - (n^2 - 1)/(2n^2 + 1)$ ^[15] and C is a constant.

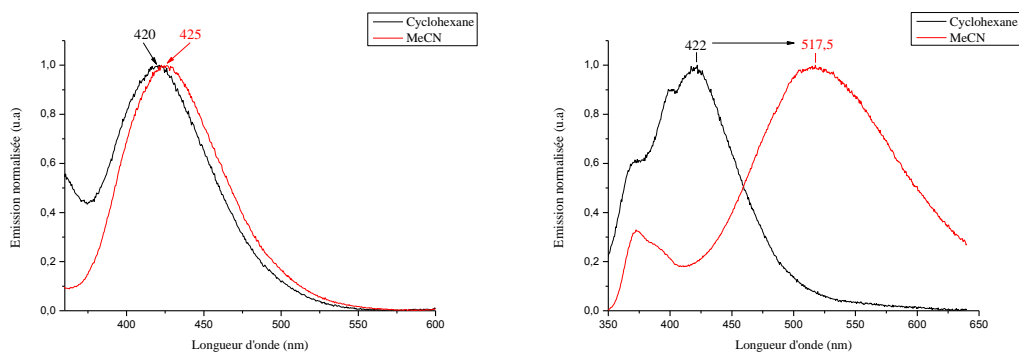
Experimentally, several points $\Delta\nu/\Delta f$ were measured from absorption and emission spectra in several solvents (Cyclohexane, Toluene, Chloroform, Ethyl Acetate, and Acetonitrile). A slope is then calculated by a linear regression on these five points and the dipole moment difference ($\Delta\mu$) is calculated with this equation:

$$\Delta\mu = \sqrt{\frac{r^3 hc \cdot \text{slope}}{2}}$$

Excited state dipole moment μ^* is then calculated from the ground state dipole moment μ estimated by DFT optimization at 6-31G(d) level of theory without solvation.

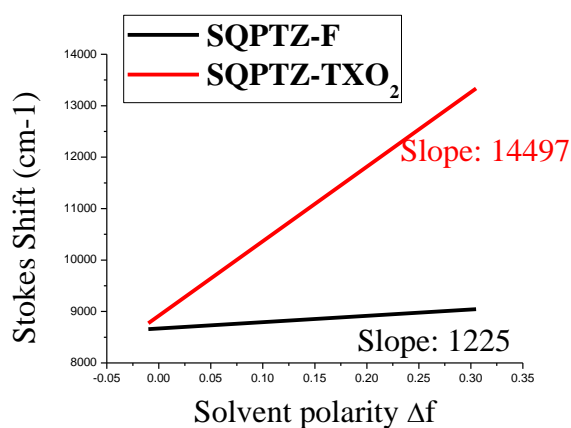


S 27 UV-Vis absorption recorded in Cyclohexane (black line) and in acetonitrile (red line) of SQPTZ-F (left) and of SQPTZ-TXO₂ (right)



S 28 Fluorescence spectra in Cyclohexane (black line) and in MeCN (red line) of SQPTZ-F (left) (λ_{exc} : 306 nm) and of SQPTZ-TXO₂ (right) (λ_{exc} : 330 nm)

Lippert-Mataga Calculations

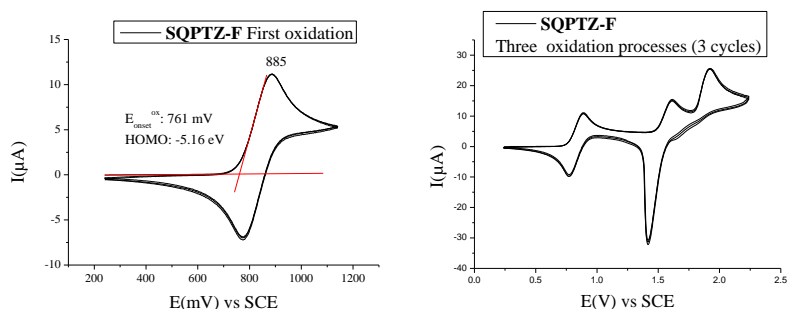


S 29 Stoke Shift (cm⁻¹) as a function of the solvent polarity Δf

	SQPTZ-F	SQPTZ-TXO₂
Δ_{Abs-Em} (cm ⁻¹) cyclohexane	8658.01	8770.85
Δ_{Abs-Em} (cm ⁻¹) CH ₃ CN	9043.88	13337.4
Slope of Stokes-Shift versus solvent polarity	1224.98	14496.98413
Molecule radius a (cm)	6.7 10 ⁻⁸	6.85 10 ⁻⁸
a ³	3.00763 10 ⁻²²	3.21419 10 ⁻²²

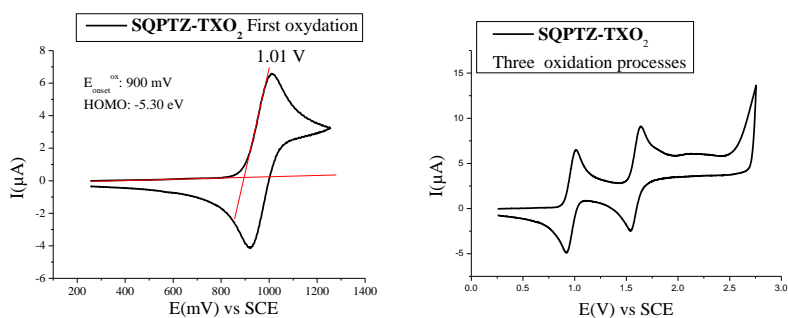
$(\text{Slope} \cdot a^3)^{1/2}$	$6.0698 \cdot 10^{-10}$	$21.586 \cdot 10^{-10}$
$\Delta\mu$ (Debye) = $\mu(S^1) - \mu(S^0) = 99.66 \cdot 10^8 (\text{slope} \cdot a^3)^{1/2}$	6.049	21.513
$\mu(S^0)$ from theoretical calculations	1.6 D	5.11
$\mu^* = \Delta\mu + \mu(S^0)$	7.5049 Debye	26.62 Debye

ELECTROCHEMICAL PROPERTIES



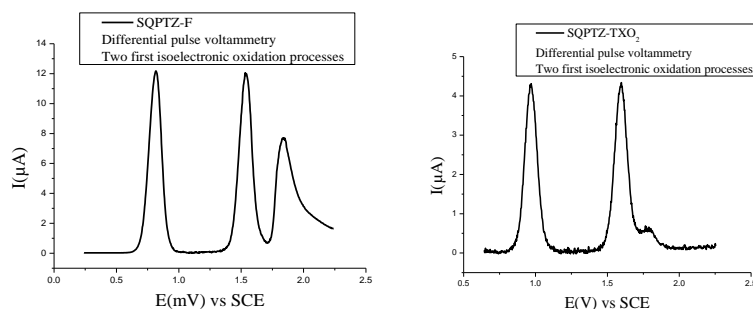
S 30 Cyclic voltammetry at 100 mV s^{-1} in $\text{CH}_2\text{Cl}_2/[\text{NBu}_4][\text{PF}_6]$ 0.2 M in presence of **SQPTZ-F** ($5 \cdot 10^{-3}$ M).

Left three recurrent sweeps on the first oxidation wave showing the reversibility of the redox process.
Right three recurrent sweeps including the three successive oxidation processes.
Platinum disk working electrode (diameter 1 mm).

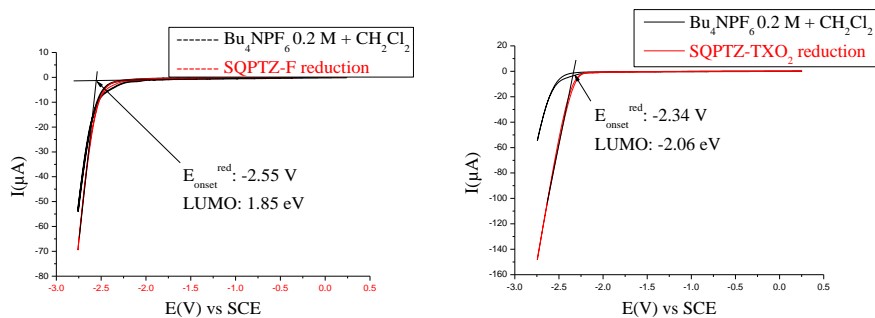


S 31 Cyclic voltammetry at 100 mV s^{-1} in $\text{CH}_2\text{Cl}_2/[\text{NBu}_4][\text{PF}_6]$ 0.2 M in presence of **SQPTZ-TXO₂** ($5 \cdot 10^{-3}$ M).

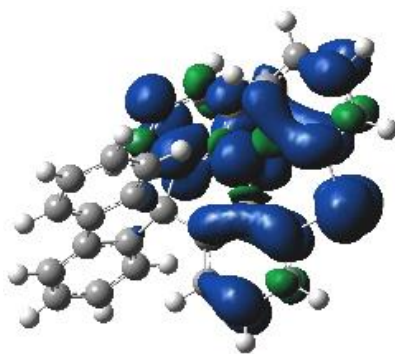
Left : first oxidation wave showing the reversibility of the redox process.
Right : three successive oxidation processes.
Platinum disk working electrode (diameter 1 mm).



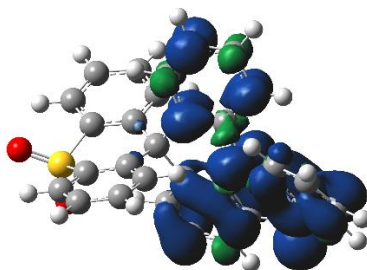
S 32 Differential pulse voltammetry in $\text{CH}_2\text{Cl}_2/[\text{NBu}_4][\text{PF}_6]$ 0.2 M in presence of **SQPTZ-F** (left) and **SQPTZ-TXO₂** (right).
Platinum disk working electrode (diameter 1 mm).



S 33 Cyclic voltammetry at 100 mV s^{-1} in $\text{CH}_2\text{Cl}_2/[\text{NBu}_4][\text{PF}_6]$ 0.2 M M in presence of **SQPTZ-F** (left) and **SQPTZ-TXO₂** (right). Platinum disk working electrode (diameter 1 mm).

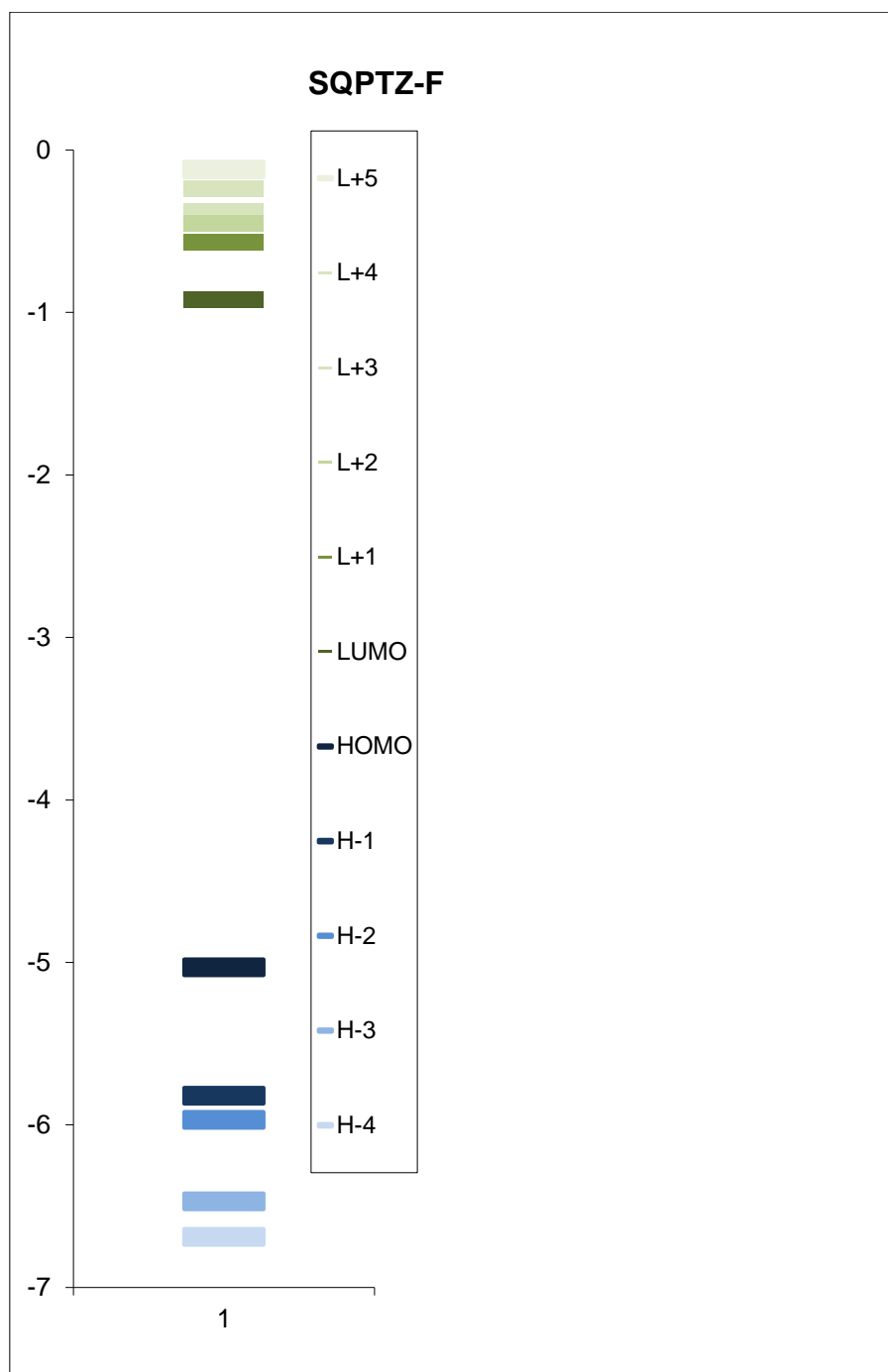


S 34 Spin density of SQPTZ-F radical cation (isovalue $0.001 \text{ e Bohr}^{-3}$)



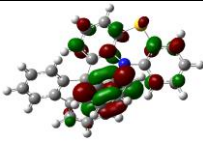
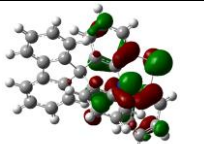
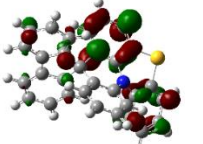
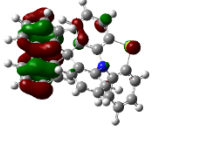

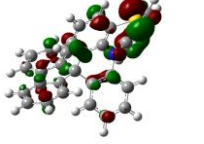
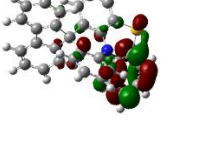
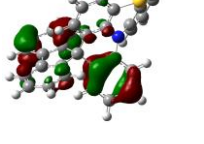
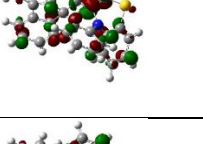
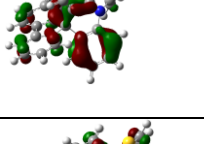

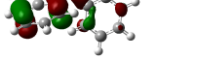
S 35 Spin density of SQPTZ-TXO₂ radical cation (isovalue $0.001 \text{ e Bohr}^{-3}$)

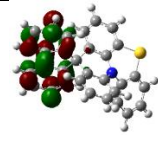
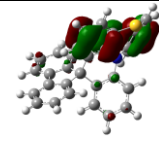
THEORETICAL MODELING



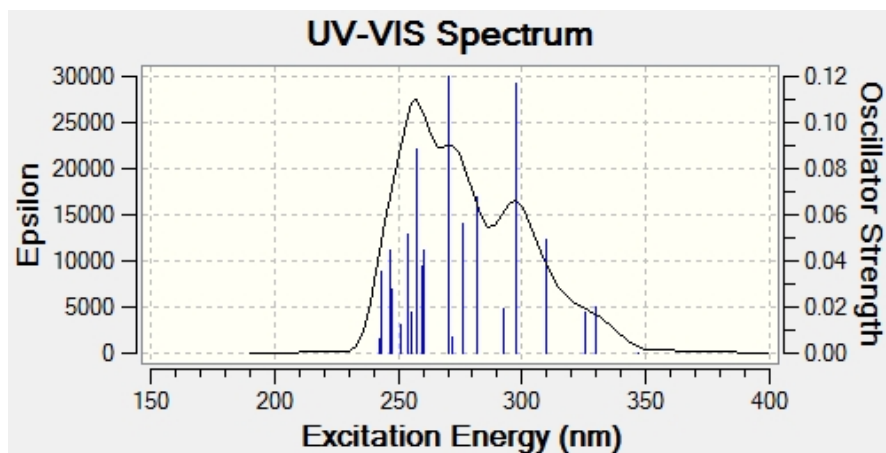
LUMO-HOMO (eV)		4.11
LUMO-HOMO (nm)		302.0746316
121	L+6	0.14 eV

120	L+5	-0.12 eV
119	L+4	-0.24 eV
118	L+3	-0.38 eV
117	L+2	-0.45 eV
116	L+1	-0.57 eV
115	LUMO	-0.92 eV
114	HOMO	-5.03 eV
113	H-1	-5.82 eV
112	H-2	-5.97 eV
111	H-3	-6.47 eV
110	H-4	-6.69 eV
109	H-5	-6.77 eV
108	H-6	-6.85 eV

MO number	Level in eV		MO number	Level in eV	
121(L+6)	0.14		114(HOMO)	-5.03	
120(L+5)	-0.12		113(H-1)	-5.82	
119(L+4)	-0.24		112(H-2)	-5.97	
118(L+3)	-0.38		111(H-3)	-6.47	
117(L+2)	-0.45		110(H-4)	-6.69	
116(L+1)	-0.57		109(H-5)	-6.77	

115(LUMO)	-0.92		108(H-6)	-6.85	
-----------	-------	---	----------	-------	---

S 36 Calculated frontier molecular orbitals of **SQPTZ-F** obtained by DFT after geometry optimization with DFT B3LYP/6-31G(d), show with an isovalue of 0.04



No.	Wavelength (nm)	Osc. Strength	Major contribs	Minor contribs
1	347.13668	0.0002	HOMO->LUMO (95%)	
2	330.0765046	0.0197	HOMO->L+1 (38%), HOMO->L+2 (47%)	HOMO->LUMO (3%), HOMO->L+3 (9%)
3	325.3472673	0.0174	HOMO->L+1 (54%), HOMO->L+2 (17%), HOMO->L+3 (25%)	

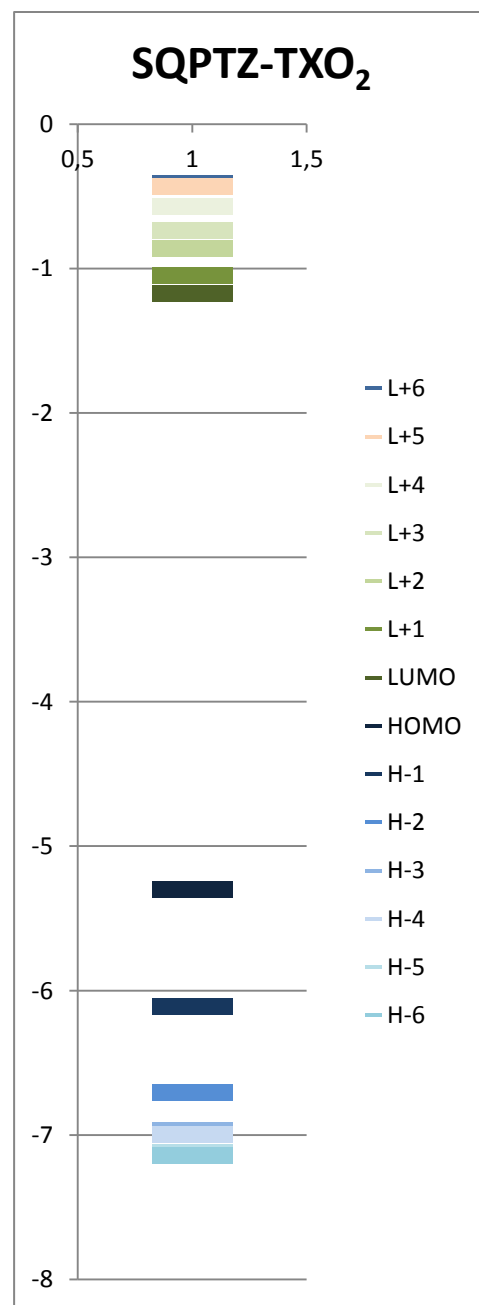
4	309.9970912	0.0492	HOMO->L+2 (31%), HOMO->L+3 (58%)	HOMO->L+1 (5%)
5	297.3078908	0.1169	HOMO->L+4 (57%), HOMO->L+5 (33%)	
6	292.6136665	0.019	HOMO->L+4 (37%), HOMO->L+5 (54%)	HOMO->L+2 (2%)
7	281.5499515	0.0674	H-1->LUMO (76%)	H-3->LUMO (6%), H-2->LUMO (7%)
8	275.8679586	0.0564	HOMO->L+6 (86%)	H-2->L+1 (3%)
9	271.7383436	0.0071	H-3->LUMO (14%), H-2->LUMO (22%), H-1->L+1 (36%), H-1->L+2 (14%)	H-1->LUMO (3%), H-1->L+3 (2%)
10	270.0279574	0.12	H-2->LUMO (65%), H-1->LUMO (11%), H-1->L+1 (16%)	H-1->L+2 (2%)
11	260.3543324	0.0445	H-1->L+1 (31%), H-1->L+2 (46%)	H-2->L+1 (5%), H-1->L+3 (3%), HOMO->L+7 (2%)
12	259.4716461	0.0376	H-2->L+1 (49%), HOMO->L+7 (11%)	H-2->L+2 (9%), H-2->L+3 (2%), H-1->L+2 (9%), H-1->L+3 (3%), H-1->L+4 (2%), HOMO->L+5 (2%)


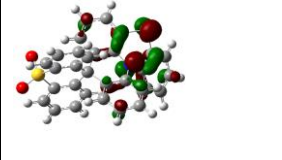
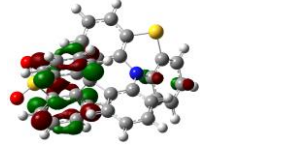
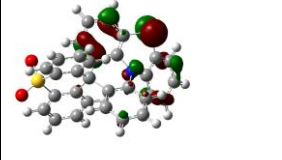
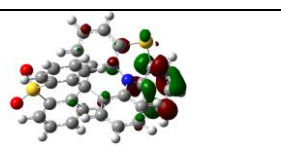
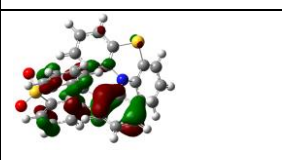
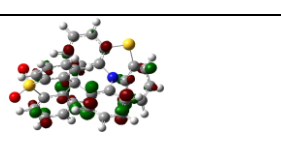
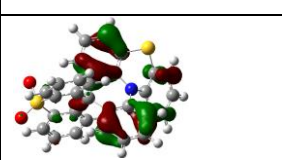
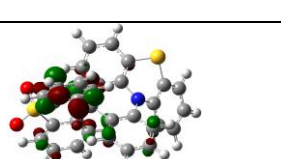
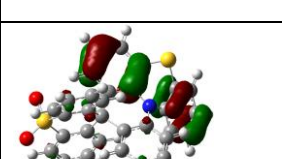
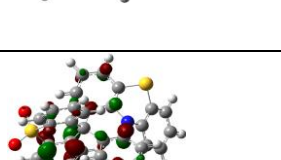
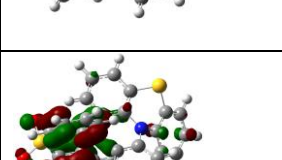
13	257.1948235	0.0881	H-2->L+1 (25%), H-2->L+2 (24%), H-1->L+3 (10%)	H-5->LUMO (5%), H-4->LUMO (4%), H-1->L+4 (7%), H-1->L+5 (7%), HOMO->L+5 (2%), HOMO->L+6 (3%), HOMO->L+7 (3%)
14	255.55144	0.0175	H-5->LUMO (13%), H-4->LUMO (12%), H-1->L+4 (31%)	H-2->L+1 (3%), H-2->L+2 (7%), H-2->L+3 (2%), H-2->L+4 (4%), H-1->L+2 (4%), H-1->L+3 (6%), H-1->L+5 (3%), H-1->L+7 (2%), HOMO->L+7 (2%)
15	253.6743461	0.0519	HOMO->L+7 (75%)	H-2->L+1 (2%), H-2->L+2 (5%), H-2->L+3 (3%), H-1->L+2 (4%), H-1->L+3 (4%)
16	251.2581551	0.0123	H-2->L+2 (37%), H-2->L+3 (11%), H-1->L+3 (42%)	
17	247.565617	0.0277	H-2->L+3 (44%), H-1->L+2 (11%), H-1->L+3	H-3->LUMO (7%), H-1->L+6 (2%), HOMO->L+8 (6%), HOMO-

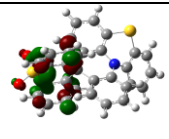
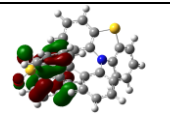
			(16%)	>L+9 (3%)
18	246.5073498	0.0449	H-3->LUMO (13%), H-2->L+3 (10%), H-1->L+4 (32%), H-1->L+5 (13%)	H-5->LUMO (4%), H-2->L+1 (2%), H-2->L+2 (5%), H-2->L+4 (3%), H-1->L+1 (3%), H-1->L+7 (2%)
19	243.0331013	0.0357	H-3->LUMO (14%), HOMO->L+8 (61%)	H-2->L+3 (3%), H-2->L+4 (3%)
20	242.6240908	0.0065	H-2->L+3 (11%), H-2->L+4 (39%), HOMO->L+9 (20%)	

S 37 Predicted UV-vis spectra from TD-DFT energy calculations of **SQPTZ-F** after geometry optimization with DFT B3LYP/6-31 G(d).

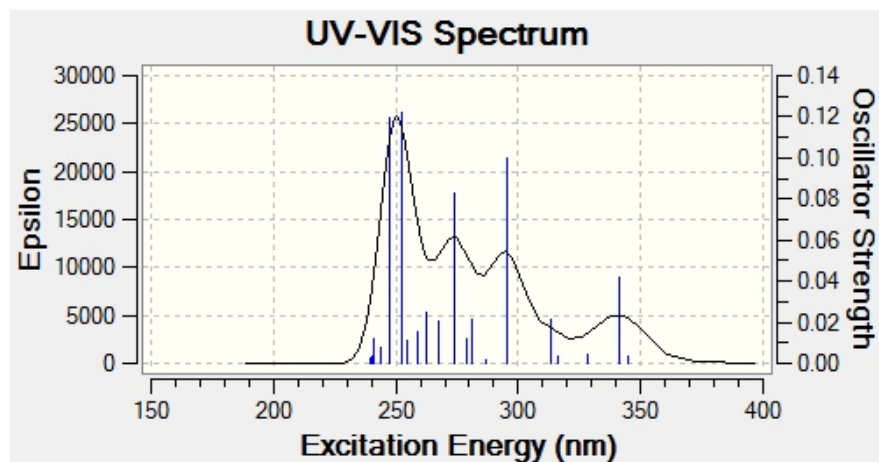
LUMO-HOMO (eV)		4.13
LUMO-HOMO (nm)		300.6118005
137	L+6	-0.3 eV
136	L+5	-0.54 eV
135	L+4	-0.65 eV
134	L+3	-0.77 eV
133	L+2	-0.87 eV
132	L+1	-1.01 eV
131	LUMO	-1.31 eV
130	HOMO	-5.31 eV
129	H-1	-6.11 eV
128	H-2	-6.24 eV
127	H-3	-6.75 eV
126	H-4	-6.98 eV
125	H-5	-7.05 eV
124	H-6	-7.13 eV



MO number	Level in eV		MO number	Level in eV	
137(L+6)	-0.3		130(HOMO)	-5.31	
136(L+5)	-0.54		129(H-1)	-6.11	
135(L+4)	-0.65		128(H-2)	-6.24	
134(L+3)	-0.77		127(H-3)	-6.75	
133(L+2)	-0.87		126(H-4)	-6.98	
132(L+1)	-1.01		125(H-5)	-7.05	

131(LUMO)	-1.31		124(H-6)	-7.13	
-----------	-------	---	----------	-------	---

S 38 Calculated frontier molecular orbitals of **SQPTZ-TXO₂** obtained by DFT after geometry optimization with DFT B3LYP/6-31G(d), show with an isovalue of 0.04



No.	Wavelength (nm)	Osc. Strength	Major contribs	Minor contribs
1	344.838785	0.0034	HOMO->LUMO (97%)	
2	341.335618	0.0418	HOMO->L+1 (96%)	
3	328.667753	0.0044	HOMO->L+2 (61%), HOMO->L+3 (22%), HOMO->L+4 (10%)	
4	315.913307	0.0031	HOMO->L+2 (33%), HOMO->L+3 (58%)	HOMO->L+4 (7%)
5	313.19205	0.021	HOMO->L+3 (15%), HOMO->L+4 (70%)	HOMO->L+6 (6%)

6	295.107078	0.0999	HOMO->L+6 (75%)	H-1->L+4 (3%), HOMO->L+4 (3%), HOMO->L+5 (9%)
7	286.633537	0.0018	HOMO->L+5 (84%), HOMO->L+6 (10%)	HOMO->L+4 (4%)
8	281.001171	0.0212	H-1->LUMO (88%)	HOMO->L+7 (4%)
9	278.676864	0.0121	H-1->L+1 (41%), HOMO->L+7 (46%)	H-1->LUMO (6%)
10	273.6939	0.0827	H-1->L+1 (49%), HOMO->L+7 (36%)	H-1->L+2 (2%), HOMO->L+6 (2%)
11	267.263067	0.0201	H-1->L+2 (41%), HOMO->L+8 (34%)	H-1->L+1 (3%), H-1->L+3 (6%), H-1->L+4 (4%), HOMO->L+6 (2%), HOMO->L+7 (3%)
12	262.810193	0.025	H-1->L+2 (49%), HOMO->L+8 (38%)	H-1->L+3 (3%), H-1->L+4 (3%)
13	258.729834	0.0155	H-1->L+3 (78%)	H-2->LUMO (5%), HOMO->L+8 (7%)
14	254.758536	0.0108	H-2->LUMO (74%)	H-6->L+2 (3%), H-1->L+3 (4%), H-1->L+4 (5%), HOMO->L+8 (3%)
15	252.645671	0.1223	H-1->L+4 (64%), HOMO->L+8 (10%)	H-4->L+1 (2%), H-2->LUMO (6%), H-2->L+1 (5%)

16	247.501371	0.1197	H-5->LUMO (10%), H-2->L+1 (47%)	H-7->L+2 (5%), H-6->L+1 (4%), H-4->LUMO (2%), H-1->L+4 (2%), H-1->L+5 (6%), H-1->L+6 (4%)
17	243.951236	0.0075	H-1->L+5 (20%), H-1->L+6 (37%)	H-6->L+1 (2%), H-5->LUMO (7%), H-4->LUMO (4%), H-2->L+1 (6%), H-2->L+2 (5%), HOMO->L+9 (4%)
18	241.245572	0.012	H-3->LUMO (12%), H-2->L+1 (16%), H-1->L+6 (37%)	H-6->L+1 (3%), H-5->LUMO (5%), H-4->LUMO (7%), HOMO->L+9 (7%)

19	240.459527	0.0031	H-1->L+5 (26%), HOMO->L+9 (36%)	H-6->L+1 (2%), H-5->LUMO (7%), H-3->LUMO (5%), H-3->L+1 (2%), H-2->L+2 (4%), H-1->L+6 (5%)
20	239.613738	0.0026	H-1->L+5 (36%), HOMO->L+9 (33%)	H-3->LUMO (2%), H-3->L+1 (5%), H-2->L+1 (2%), H-1->L+4 (3%), H-1->L+6 (6%), HOMO->L+10 (3%)

S 39 Predicted UV-vis spectra from TD-DFT energy calculations of **SQPTZ-TXO₂**, after geometry optimization with DFT B3LYP/6-31 G(d).

ORGANIC LIGHT EMITTING DIODES

OLED structure:

Glass/ITO/CuPc 10nm/ α -NPB 40nm/TCTA 10nm/ **SQPTZF** : FIrpic: 10% 20nm/TmPyPB 50nm/ LiF 1,2nm/Al 100nm.

ITO: Indium Tin Oxide: anode

CuPc: copper phthalocyanine: hole injecting layer

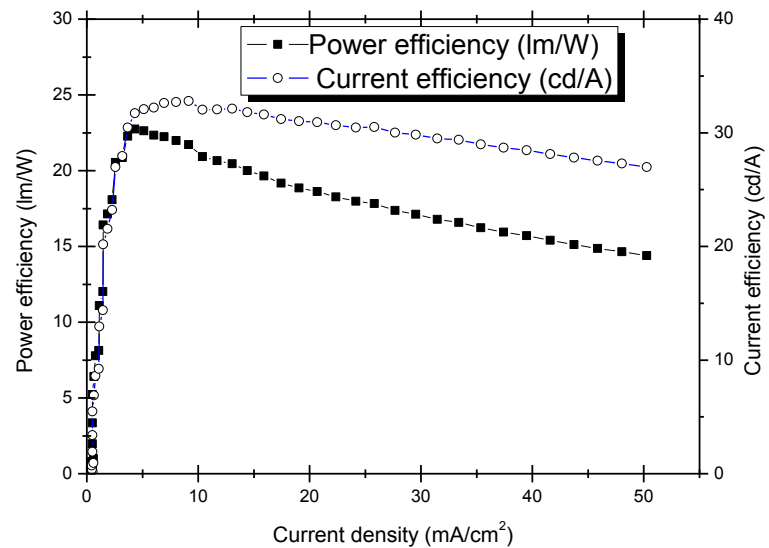
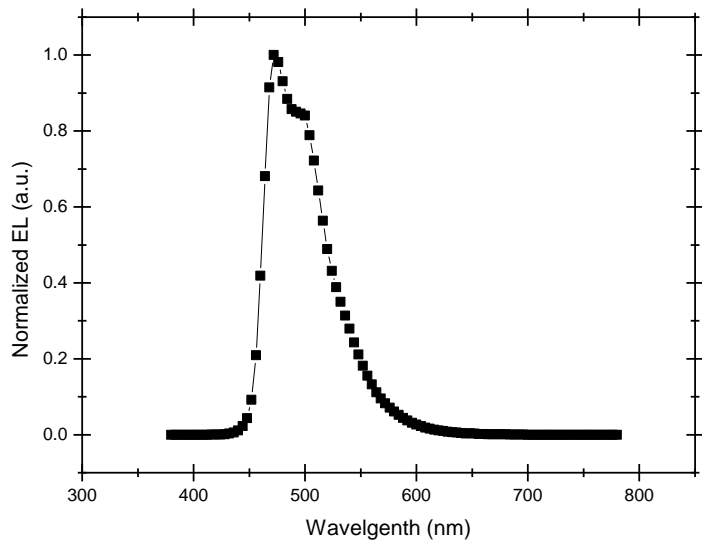
NPB: N,N'-di(1-naphthyl)-N,N'-diphenyl-[1,10-biphenyl]-4,4'-diamine: hole transporting layer

TCTA: 4,4',4''-tris(carbazole-9-yl)triphenylamine: electron/exciton blocking layer

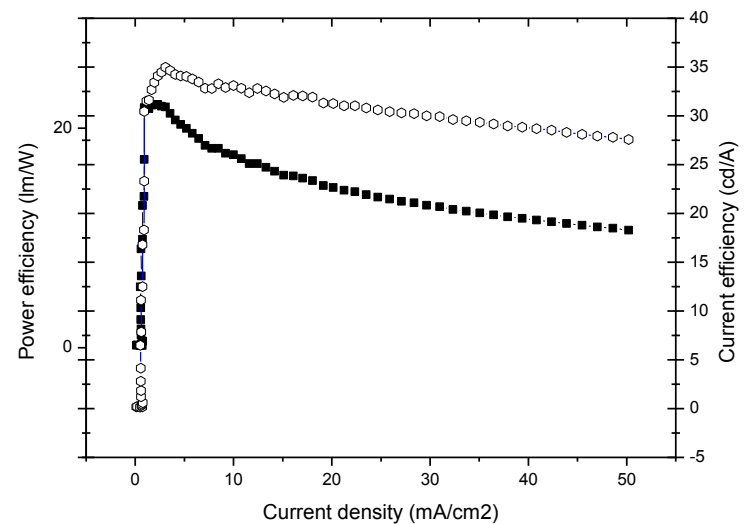
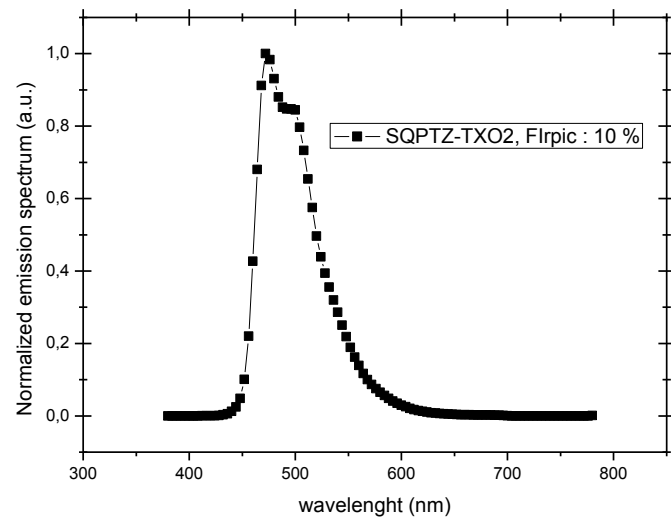
TmPyPB: 1,3,5-Tris(3-pyridyl-3-phenyl)benzene: electron transport/hole blocking layer

LiF/Al: Lithium fluoride covered with aluminum is the cathode

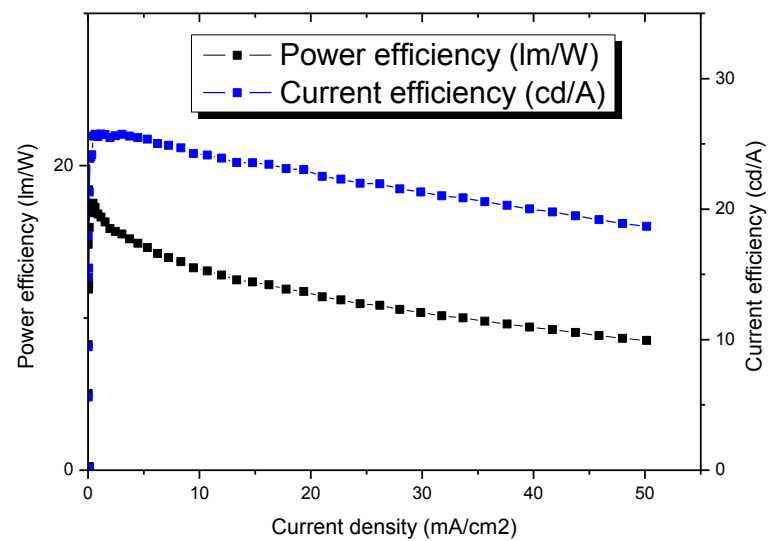
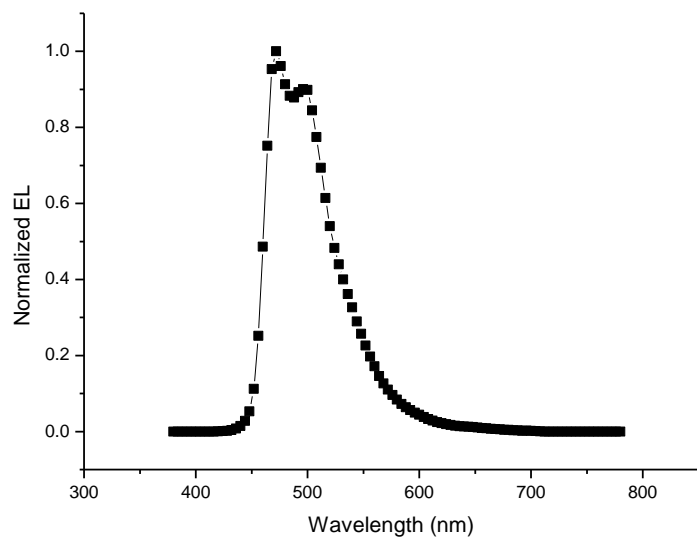
Firpic: Bis[2-(4,6-difluorophenyl)pyridinato- C^2, M](picolinato)iridium(III), blue phosphorescent emitter, $E_T = 2.62$ eV



S 40 Normalized EL, power and current efficiencies of the diode with 10% in mass of FIrpic in **SQPTZ-F** as a function of the current density.



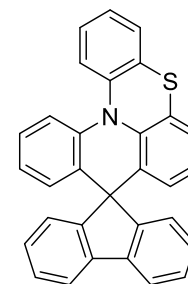
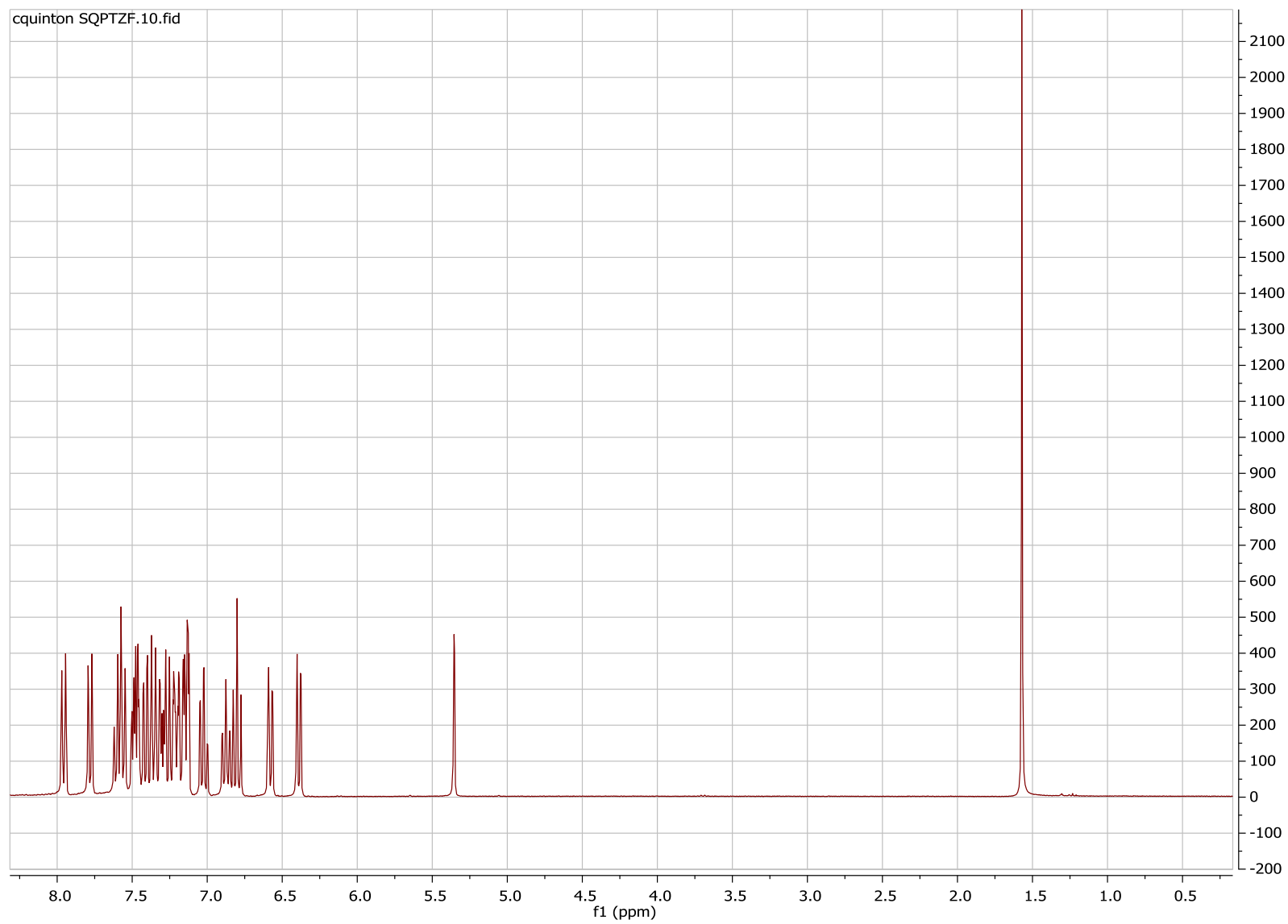
S 411 Normalized EL, power and current efficiencies of the diode with 10% in mass of FIrpic in **SQPTZ-TXO₂** as a function of the current density.

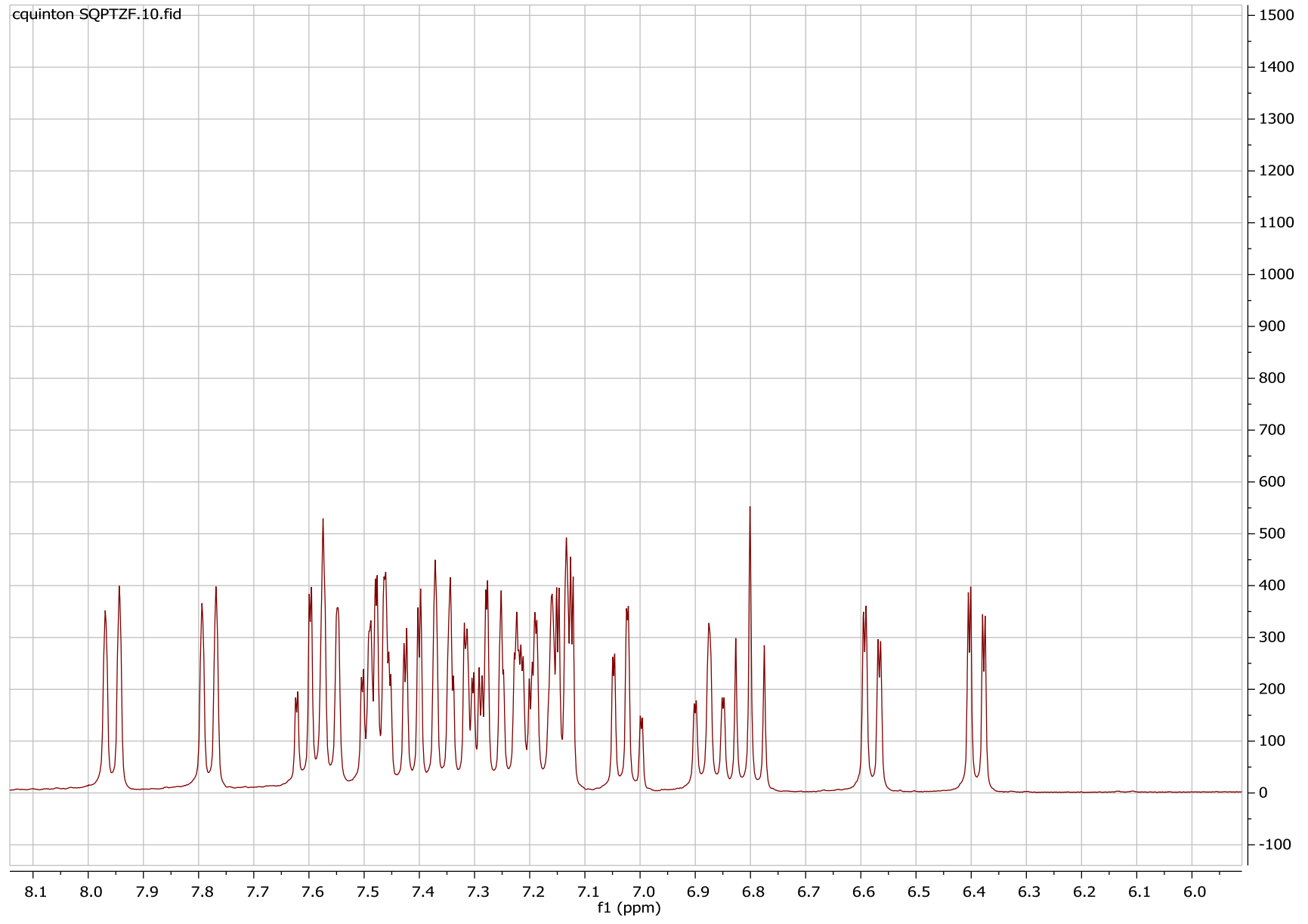


S 42 Normalized EL, power and current efficiencies of the diode with 10% in mass of FIRpic in **SIA-F** as a function of the current density.

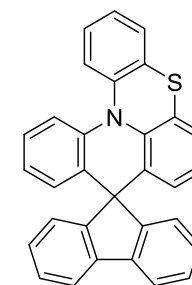
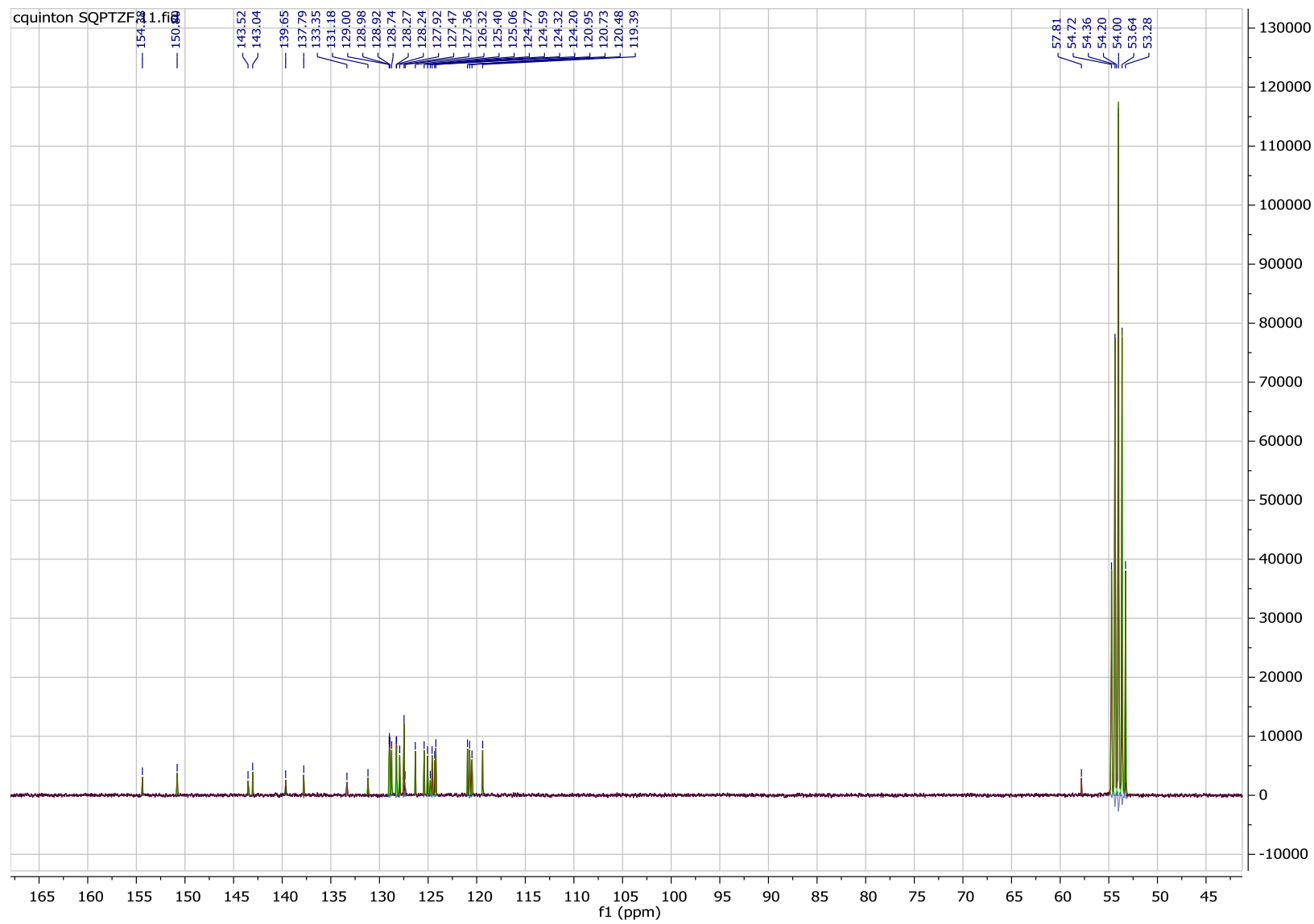
COPIES OF NMR SPECTRA

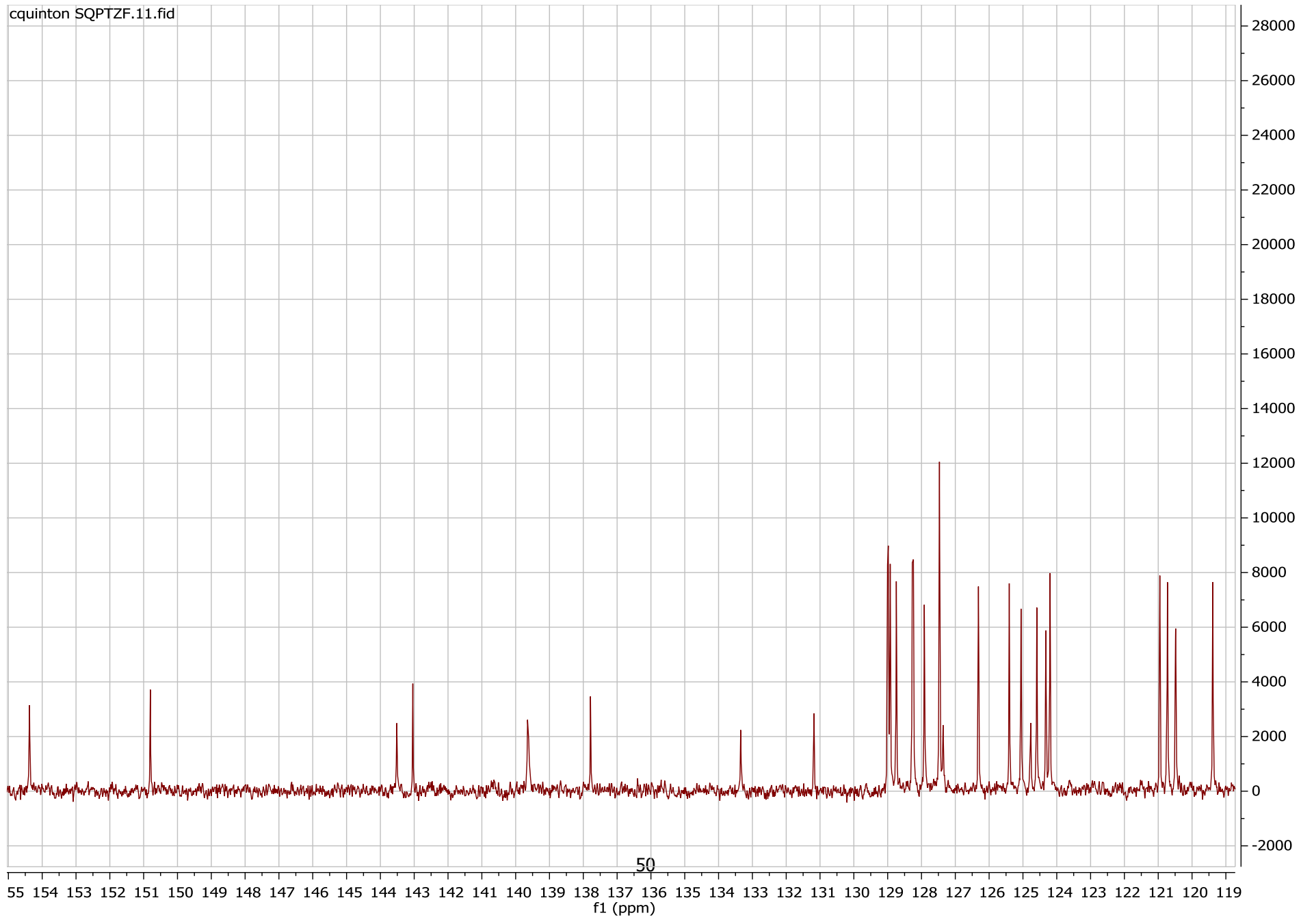
^1H -(SQPTZ-F)- CD_2Cl_2



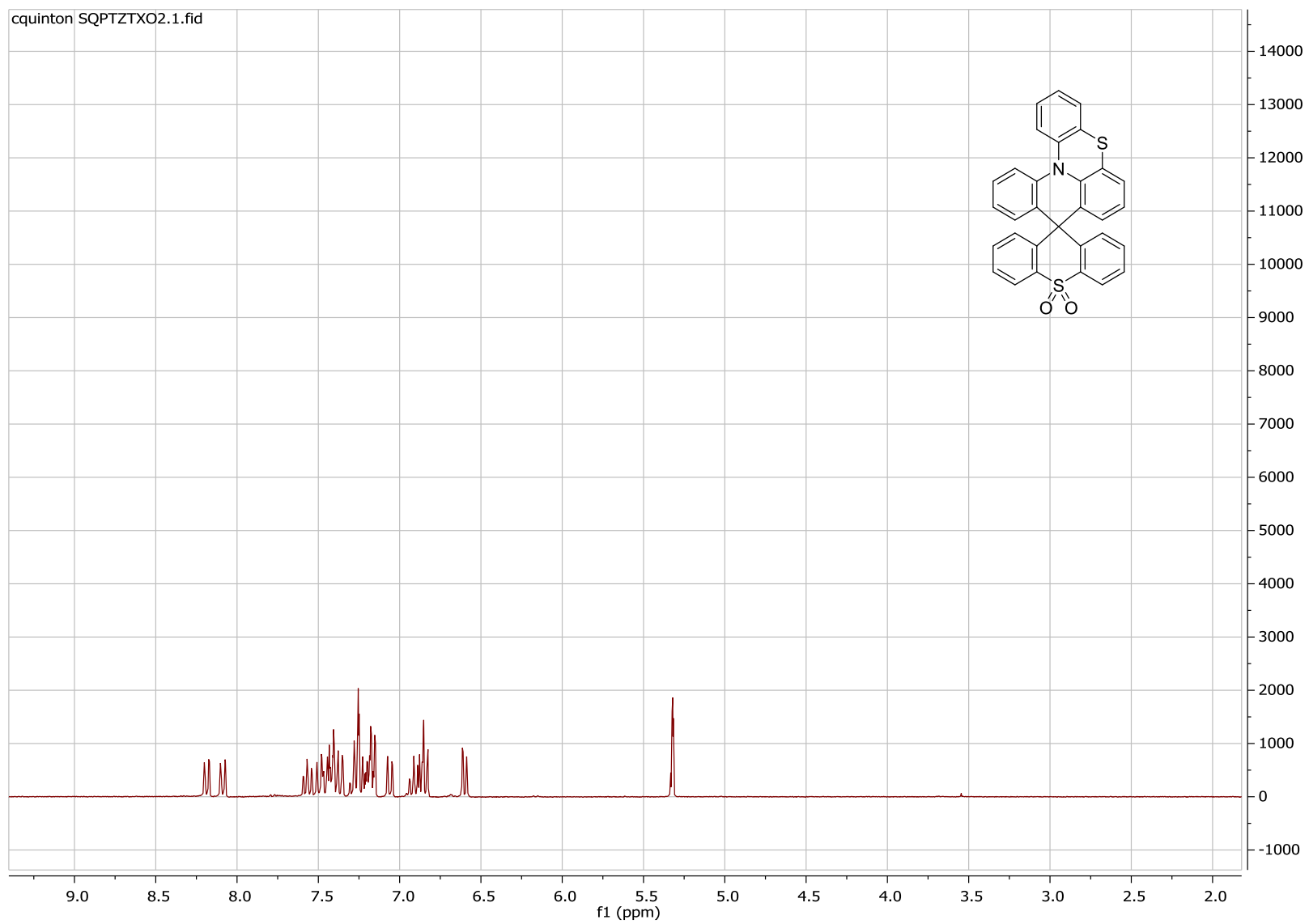


¹³C-(SQPTZ-F)-CD₂Cl₂

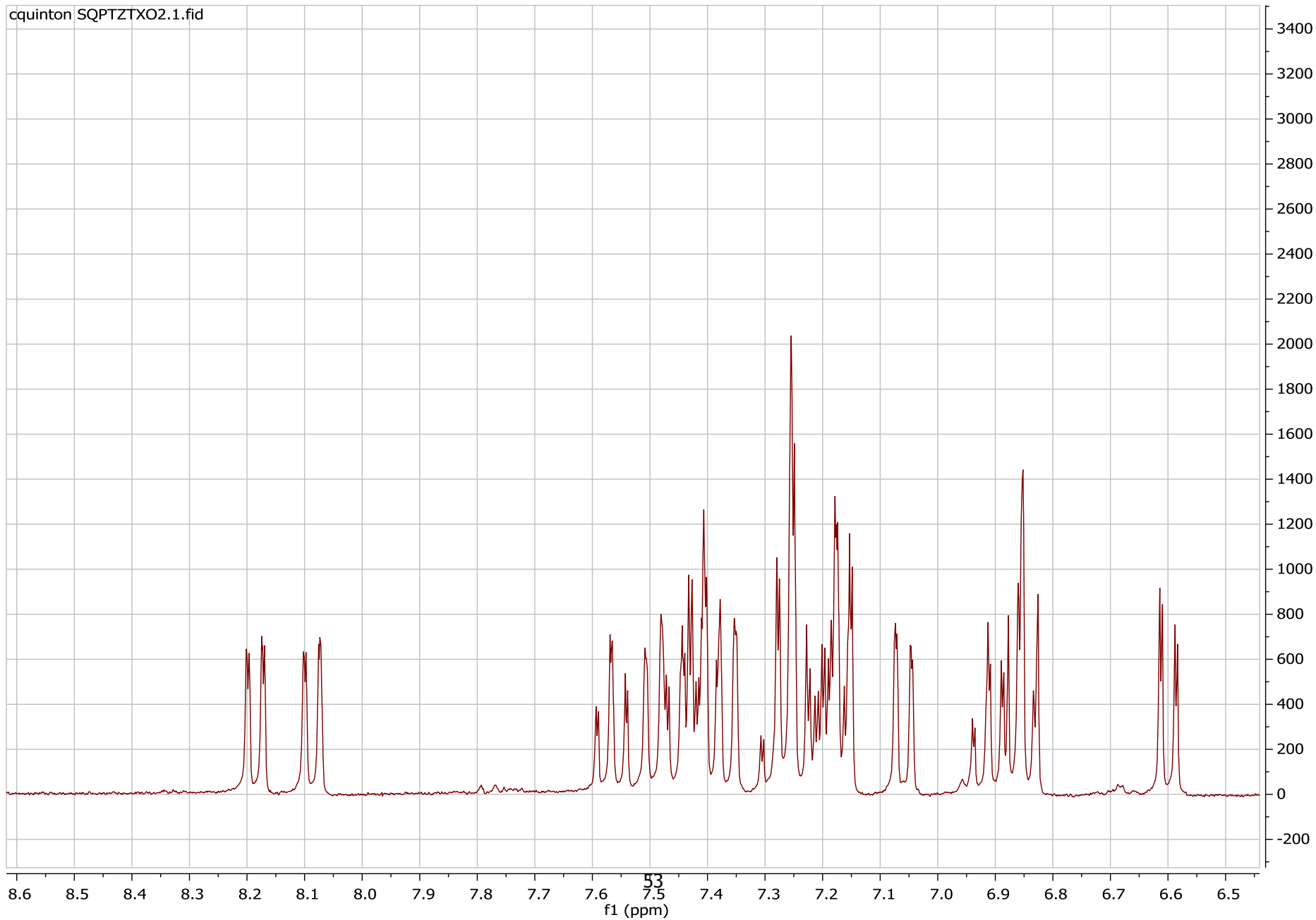




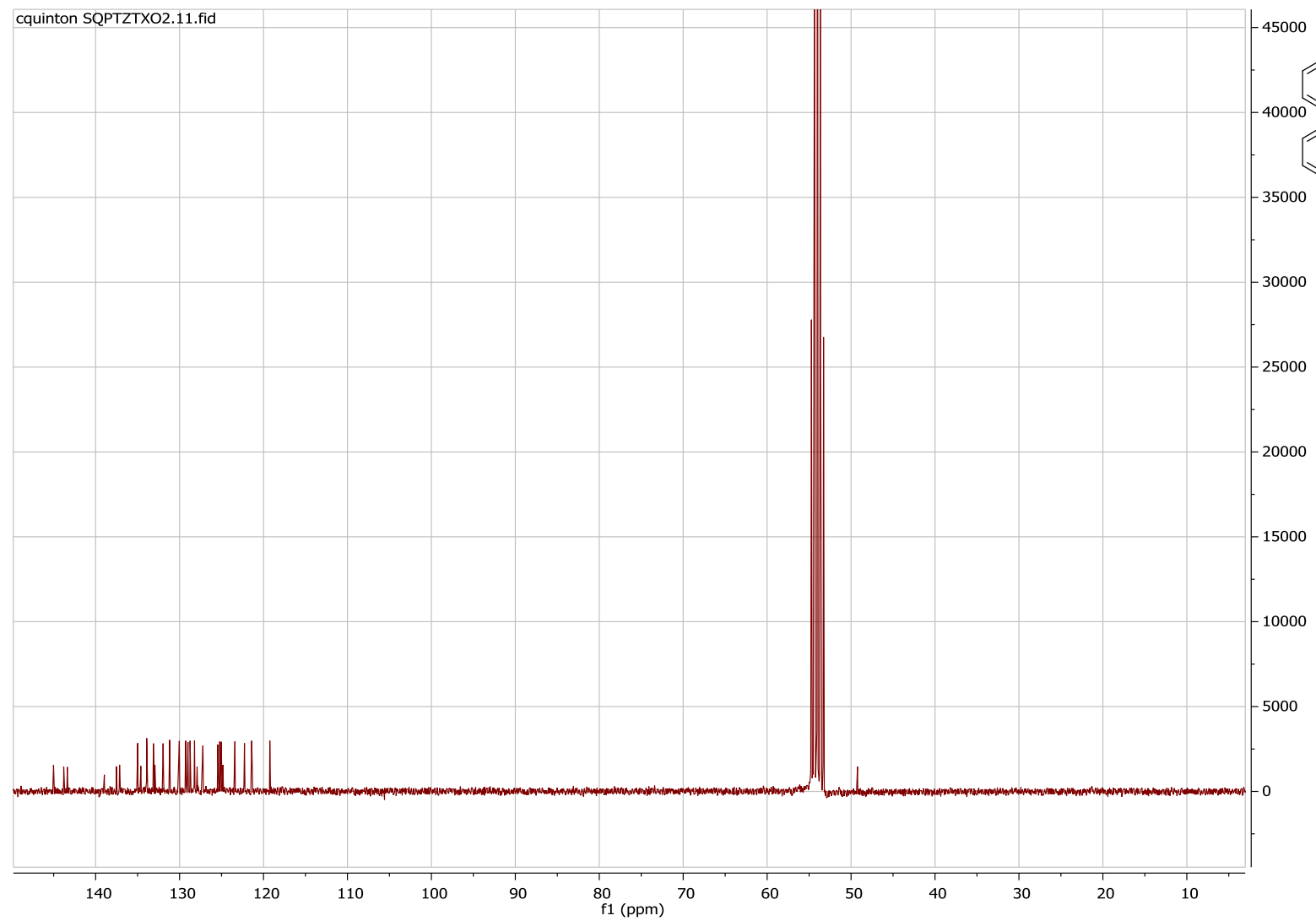
^1H -**(SQPTZ-TXO₂)**-CD₂Cl₂

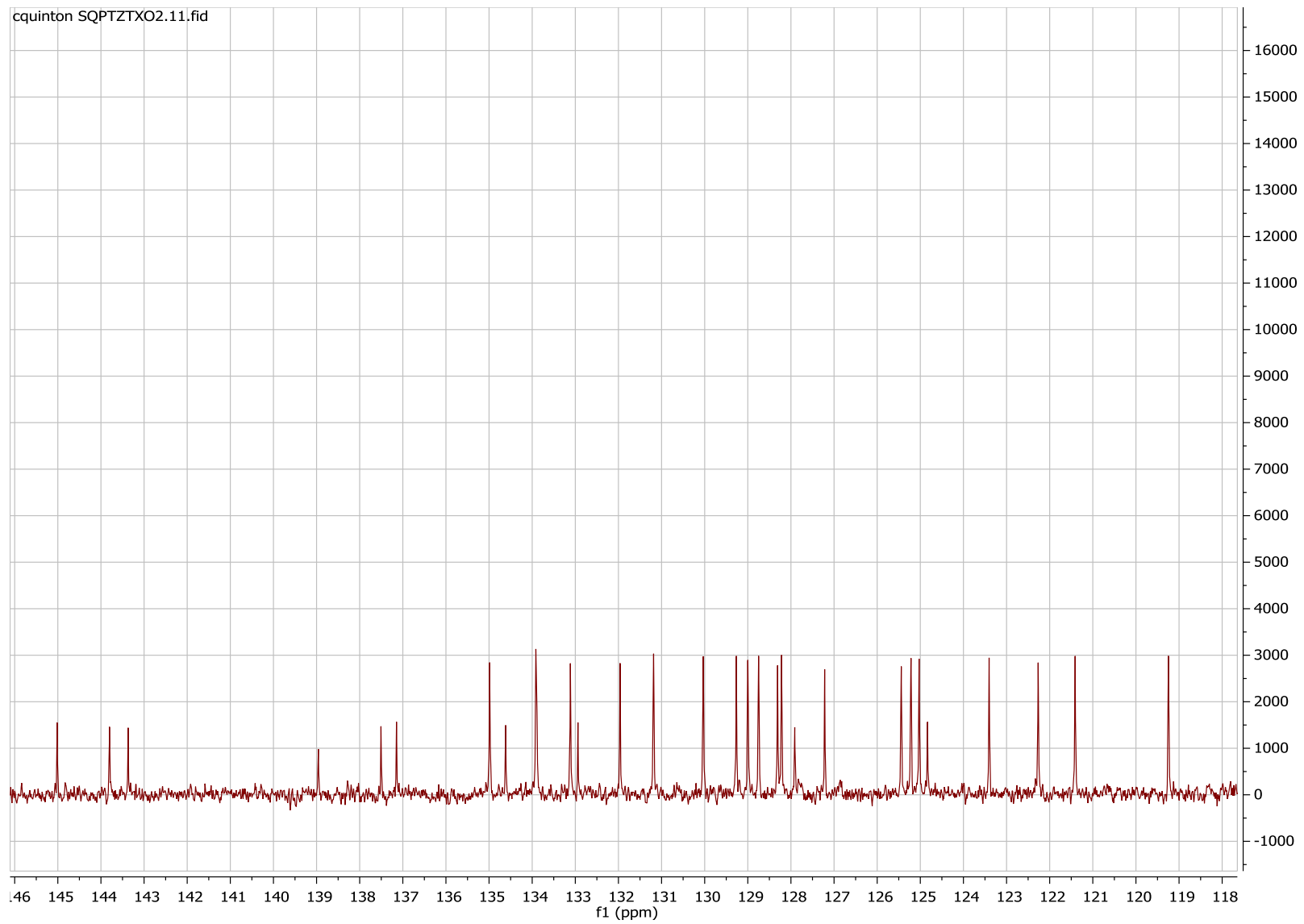


cquinton SQPTZTXO2.1.fid

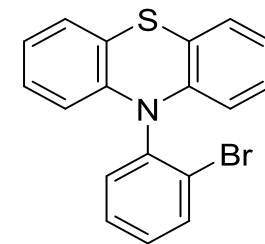
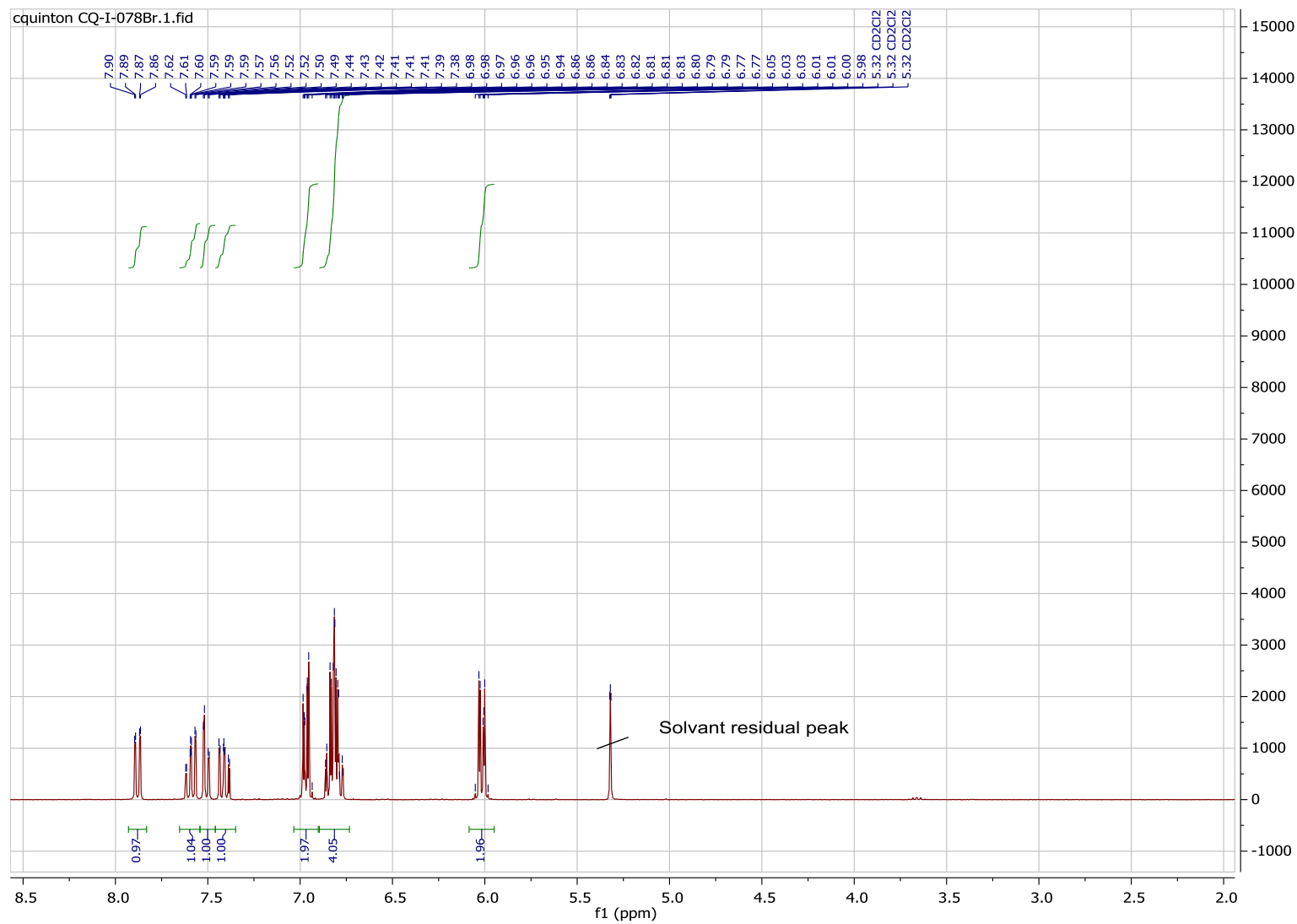


^{13}C -(SQPTZ-TXO₂)-CD₂Cl₂

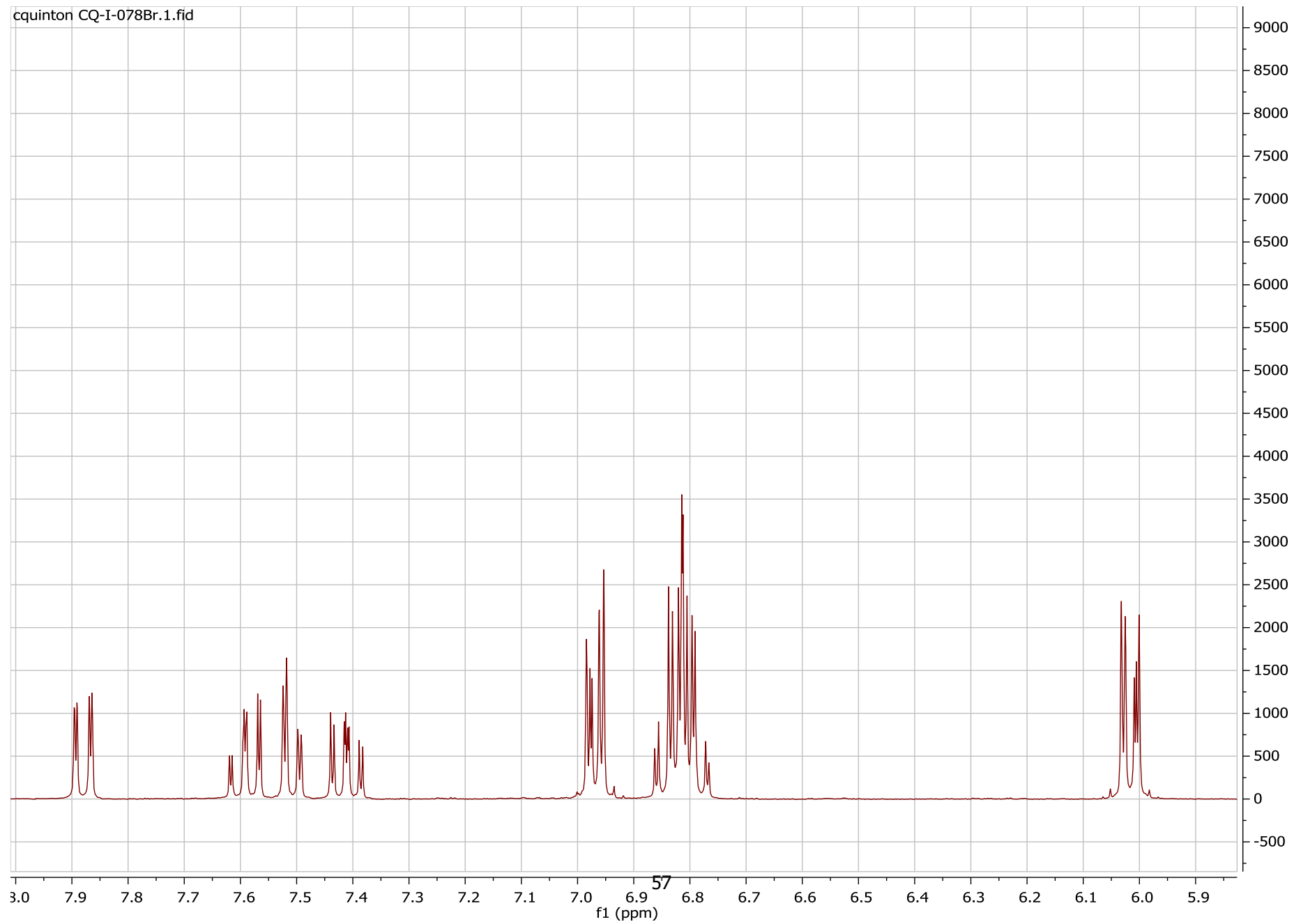




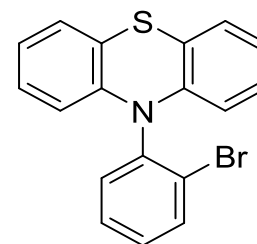
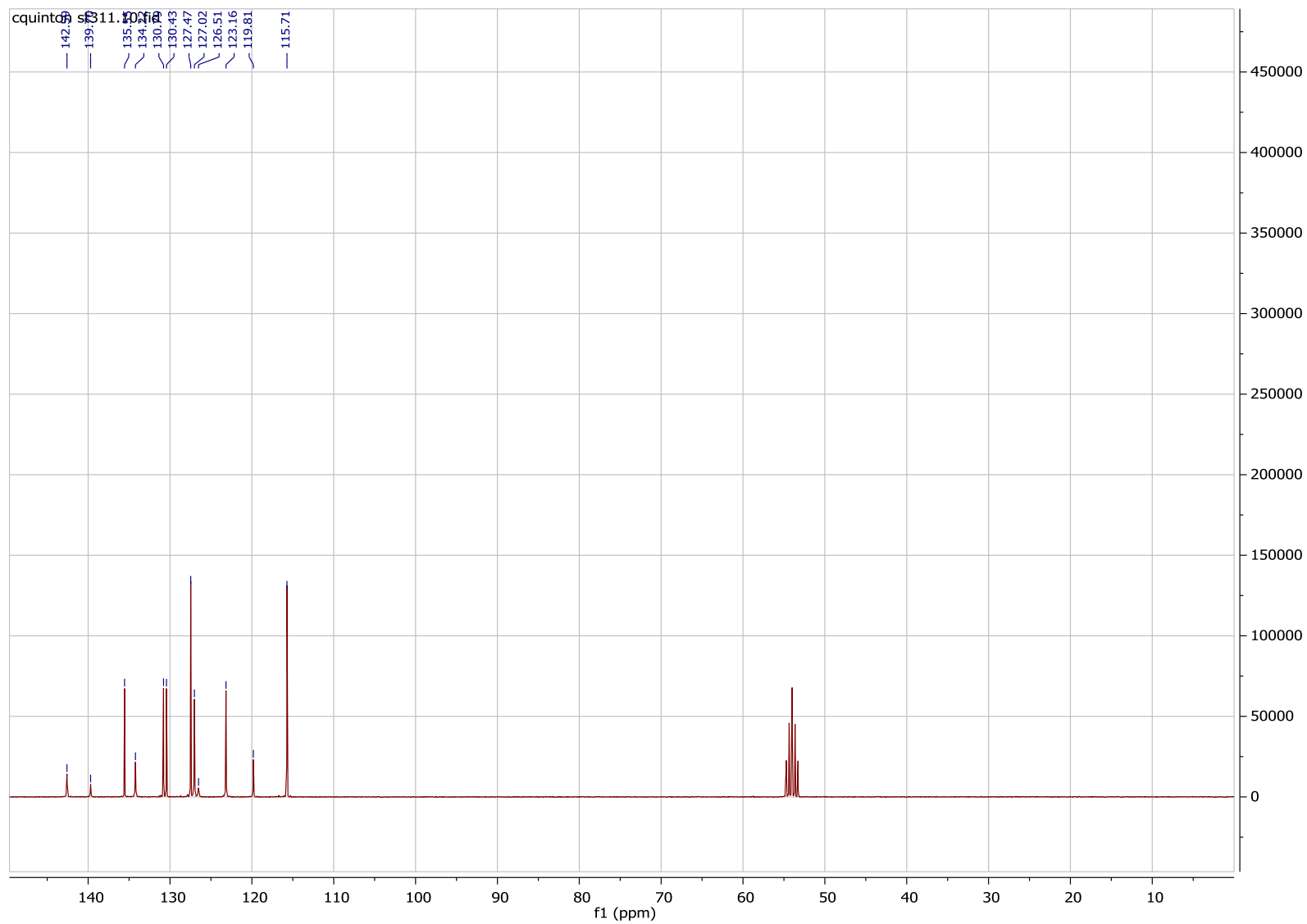
^1H -(**1**)- CD_2Cl_2

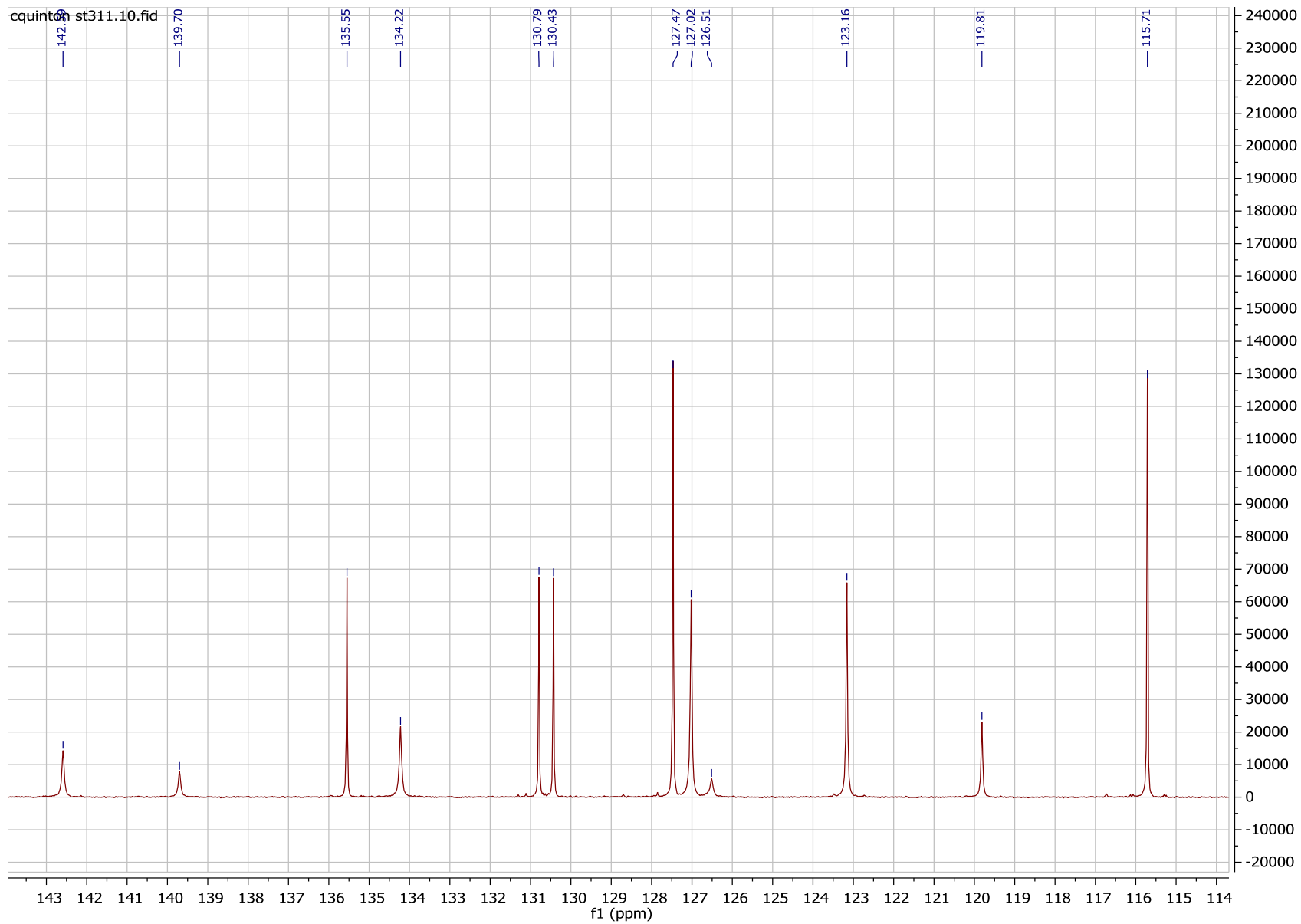


cquinton CQ-I-078Br.1.fid



^{13}C -(1)- CD_2Cl_2





REFERENCES

- [1]A. Altomare, M. C. Burla, M. Camalli, G. Cascarano, C. Giacovazzo, A. Guagliardi, A. G. G. Moliterni, G. Polidori, R. Spagna, *J. Appl. Cryst.* **1999**, *32*, 115.
- [2]L. J. Farrugia, *J. Appl. Cryst.* **2012**, *45*, 849.
- [3]A. P. Kulkarni, C. J. Tonzola, A. Babel, S. A. Jenekhe, *Chem. Mater.* **2004**, *16*, 4556.
- [4]C. M. Cardona, W. Li, A. E. Kaifer, D. Stockdale, G. C. Bazan, *Adv. Mater.* **2011**, *23*, 2367.
- [5]P. Hohenberg, W. Kohn, *Phys. Rev.* **1964**, *136*, B864.
- [6]J.-L. Calais, *Int. J. Quantum Chem.* **1993**, *47*, 101.
- [7]A. D. Becke, *Phys. Rev.* **1988**, *38*, 3098.
- [8]A. D. Becke, *J. Chem. Phys.* **1993**, *98*, 1372.
- [9]A. D. Becke, *J. Chem. Phys.* **1993**, *98*, 5648.
- [10]C. Lee, W. Yang, R. G. Parr, *Phys. Rev. B* **1988**, *37*, 785.
- [11]M. J. Frisch, G. W. Trucks, H. B. Schlegel, G. E. Scuseria, M. A. Robb, J. R. Cheeseman, R. Scalmani, G. Barone, B. Mennucci, G. A. Petersson, H. Nakatsuji, M. Caricato, X. Li, H. P. Hratchian, A. F. Izmaylov, J. Bloino, G. Zheng, J. L. Sonnenberg, M. Hada, M. Ehara, K. Toyota, R. Fukuda, J. Hasegawa, M. Ishida, T. Nakajima, Y. Honda, O. Kitao, H. Nakai, T. Vreven, J. A. J. Montgomery, J. E. Peralta, F. Ogliaro, M. Bearpark, J. J. Heyd, E. Brother, K. N. Kudin, V. N. Staroverov, R. Kobayashi, J. Normand, K. Raghavachari, A. Rendell, J. C. Burant, S. S. Iyengar, J. Tomasi, M. Cossi, N. Rega, N. J. Millam, M. Klene, J. E. Knox, C. Pomelli, J. W. Ochterski, R. L. Martin, K. Morokuma, V. G. Zakrzewski, G. A. Voth, P. Salvador, J. J. Dannenberg, S. Dapprich, A. D. Daniels, O. Farkas, J. B. Foresman, J. V. Ortiz, J. Cioslowski, D. J. Fox, *Gaussian 09, version A02, Gaussian, Inc., Wallingford, CT, 2009.* **2009**
- [12]E. Lippert, *Zeitschrift für Naturforschung* **1955**, 541.
- [13]Y. Ooshika, *J. Phys. Soc. Jpn.* **1954**, *9*, 594.
- [14]N. Mataga, Y. Kaifu, M. Koiz, *Bull. Chem. Soc. Jpn.* **1956**, *29*, 456.
- [15]W. M. Haynes, *CRC Handbook of Chemistry and Physics*, **2011**.